A New Na^+-Specific DNAzyme Mutant from *in Vitro* Selection

by

Lingzi Ma

A thesis
presented to the University of Waterloo
in fulfilment of the
thesis requirement for the degree of
Master of Science
in
Chemistry

Waterloo, Ontario, Canada, 2017

Author's Declaration

I hereby declare that I am the sole author of this thesis. This is a true copy of the thesis, including any required final revisions, as accepted by my examiners.

I understand that my thesis may be made electronically available to the public.

Abstract

Sodium is one of the most ubiquitous metal ions in both intracellular and extracellular fluids. Many fluorescent sensors have been designed to measure Na^+ concentrations. However, Na^+ binding to biomolecules such as DNA has long been considered to be non-specific. In the past few years, RNA-cleaving DNAzymes have emerged as promising tools for detecting Na^+ due to their metal-specific activity. DNAzymes are DNA-based catalysts which require specific metal ions as cofactors for their catalytic activity. The initial goal of this research is to select DNAzymes that require $Co(NH_3)_6^{3+}$ as an intended cofactor through *in vitro* selection. However, new mutants of a previously reported Na^+-specific DNAzyme were obtained instead.

An *in vitro* selection was preformed following a standard protocol using $Co(NH_3)_6^{3+}$ as the intended cofactor. After 6 rounds of selection in pH 6 buffer, an active sequence was successfully enriched and isolated. However, this sequence named CoH1 shows catalytic activity in the presence of Na^+, instead of $Co(NH_3)_6^{3+}$. The secondary structure prediction revealed a well-defined Na^+ binding domain in its catalytic core, which explained the Na^+-dependent activity. After a careful comparison, the structure of CoH1 was found to be highly similar to a previously reported Na^+-dependent DNAzyme, NaA43. However, two nucleotides in NaA43 that are known to be critical for its activity were mutated to different bases in CoH1. Indeed, further mutation studies indicated that any changes to these mutated positions may completely abolish the activity of CoH1.

As a new mutant of NaA43, CoH1 exhibited novel catalytic activity. With 10 mM Na^+, CoH1 displays a fast cleavage rate of ~0.07 min^{-1}, which is ~3.5-fold higher than NaA43. At pH 6, CoH1 has a stronger Na^+-binding affinity with a K_d value of 4.3 ± 0.6 mM Na^+, suggesting a great potential in Na^+ detection at low concentrations. Based on our results, pH is important for

distinguishing CoH1 from NaA43. Overall, CoH1 displays higher cleavage activity at pH below ~6.5, while NaA43 is more active at higher pH.

In addition, 2-aminopurine (2AP) was used as a fluorescence probe in converting the CoH1 DNAzyme into a folding-based Na^+ sensor. 2AP is a fluorescent adenine analog whose fluorescence is strongly dependent on its local base stacking environment. By introducing a 2AP in the substrate strand, binding of Na^+ induces ~80% signal enhancement. The Na^+ sensor was demonstrated to be highly sensitive (a detection limit of 3.0 mM Na^+) and selective over other monovalent ions. The 2AP probes also revealed the Na^+-induced folding of the DNAzyme and provided important insights to the reaction mechanism.

Acknowledgements

First of all, I would like to express my heartfelt gratitude to my supervisor, Dr. Juewen Liu, for his warm-hearted encouragement and most valuable advice, especially for his continual guidance and insightful comments on this research project. I would also like to express great appreciation to my committee members: Dr. Guy Guillemette and Dr. Thorsten Dieckmann for their advice and time given to evaluate my research project. In addition, I would like to acknowledge Cathy van Esch for her kind guidance.

My sincere thanks also go to every group member in the Liu lab: Po-Jung Jimmy Huang, Biwu Liu, Runjhun Saran, Wenhu Zhou, Zhicheng Huang, Zijie Zhang, Anand Lopez, Yibo Liu, and Tianmeng Yu, for their friendly suggestion and warm-hearted help in work, most importantly for their sincere solicitude and love in my life. I am extremely grateful for the encouragement and support given by my dear families.

Finally, I would like to thank University of Waterloo, the Department of Chemistry for financial support and all the research equipment.

Table of contents

List of figures

List of tables

List of abbreviations

2AP	2-aminopurine
A	adenine
APS	ammonium persulfate
C	cytosine
CD	circular dichroism
DMS	dimethyl sulfate
DNA	deoxyribonucleic acid
DNAzyme	deoxyribozyme
dNTP	deoxynucleotide
dPAGE	denaturing polyacrylamide gel electrophoresis
EDTA	ethylenediaminetetraacetic acid
ESI MS	electrospray ionization mass spectrometry
FAM	6-carboxyfluorescein
G	guanine
HEPES	2-[4-(2-hydroxyethyl)piperazin-1-yl]ethanesulfonic acid
*K*d	apparent dissociation constant

MES	2-(N-morpholino)ethanesulfonic acid
NAEs	nucleic acid enzymes
NMR	nuclear magnetic resonance
nt	nucleotide
PCR	polymerase chain reaction
rA	ribo-adenosine
RNA	ribonucleic acid
rt-PCR	real-time polymerase chain reaction
SELEX	systematic evolution of ligands by exponential enrichment
T	thymine
TBE	Tris/Borate/EDTA
TEMED	tetramethylethylenediamine
Tris	tris(hydroxymethyl)aminomethane
U	uracil

Chapter 1. Introduction

1.1 Nucleic acids

Along with carbohydrates, lipids, and proteins, nucleic acids are among the most important biological macromolecules in all forms of life. Within cells, nucleic acids, including deoxyribonucleic acid (DNA) and ribonucleic acid (RNA), function in preserving, transmitting and expressing genetic information. Essentially, DNA and RNA are linear biopolymers with nucleotides as their repeating units. The three essential components of a nucleotide are: a) a five-membered sugar ring; b) a nucleobase linked to the 1′-carbon on the sugar ring; and c) a phosphate group at the 5′-carbon (Figure 1.1A). The major difference between the DNA and RNA structure lies in the sugar ring: DNA contains 2′-deoxyribose while RNA contains ribose. DNA uses four nucleobases: adenine (A), thymine (T), cytosine (C), and guanine (G). On the contrary, RNA uses uracil (U) instead of thymine (Figure 1.1B). The neighbouring nucleotides are connected through the phosphodiester linkage between the 3′-hydroxyl group of one nucleotide and 5′-phosphate group of the next.

Resulting from Watson-Click base pairing, naturally occurring DNAs are found primarily in the double-stranded structure. Two complementary strands are held together by hydrogen bonds formed between intramolecular base pairs. Resulting from the low pK_a value of the phosphate group (pK_{a1}=2.2), the DNA backbone is negatively charged at neutral pH (pH 7.0). The alternating phosphate group and sugar residues construct the DNA backbone. The genetic information carried by DNA is stored in the sequence of base pairs and protected by the DNA backbone. Due to its genetic function in biology, DNA has been considered as a chemically passive molecule for a long time.

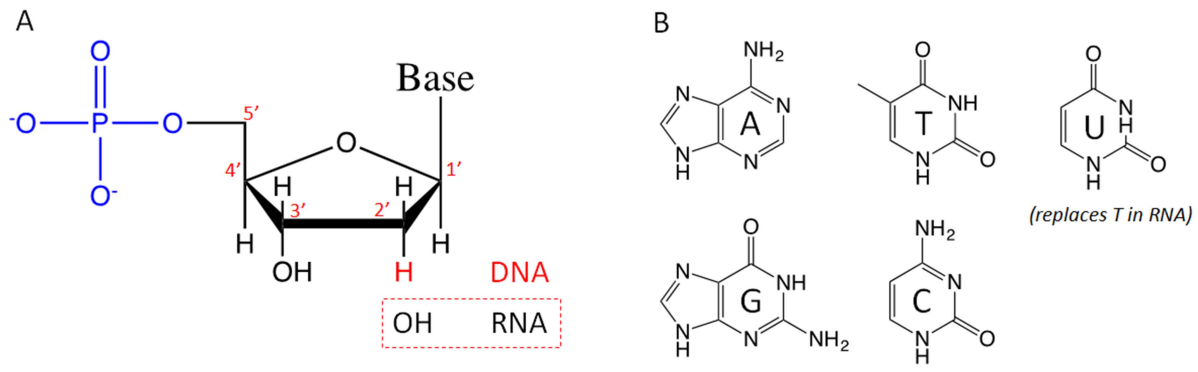

Figure 1.1 (A) The chemical structure of nucleotides and (B) the five nucleobases (A, T, C, G, U).

1.2 Introduction to DNAzymes

1.2.1 Catalytic DNA

Far beyond their roles as genetic information carriers, some nucleic acids are cable of catalyzing biochemical reactions similar to protein enzymes, which are called nucleic acid enzymes (NAEs). RNA-based catalysts or ribozymes were first discovered in the early 1980s.[1] Ever since, natural ribozymes have been found to participate in several fundamental reactions, such as RNA cleavage,[2] RNA self-processing,[3] and peptide bond formation.[4] Their DNA counterparts, deoxyribozymes or DNAzymes, are DNA molecules with catalytic activity toward specific chemical reactions. Despite the lack of known DNAzymes in nature, the first artificial DNAzyme (GR-5) was isolated through *in vitro* selection in 1994 by Breaker and Joyce.[5] This DNAzyme succeeded in catalyzing the cleavage of a RNA substrate in the presence of Pb^{2+}.

The discovery of the GR-5 DNAzyme demonstrated that DNA can exhibit catalytic activity. Since then, many DNAzymes have been identified to catalyze a great variety of chemical reactions including RNA/DNA cleavage,[6-7] ligation,[8] DNA phosphorylation,[9] and DNA adenylation.[10] Among these, DNA-catalyzed RNA cleavage reaction is the most commonly

studied. For example, Figure 1.2 shows the catalytic motif of the first RNA-cleaving DNAzyme (GR-5) which contains 15 nucleotides.[5] The enzyme strand consists of two substrate binding domains flanking a catalytic core. Substrate binding domains recognize and hybridize with the substrate strand by base pairing, yielding a DNAzyme complex. A ribo-adenosine (rA) embedded in the substrate sequence indicates the cleavage site. The GR-5 DNAzyme exhibited a catalytic rate up to ~1 min^{-1} in the presence of Pb^{2+} at 23℃ and pH 7. This rate is about 10^5-fold higher than the uncatalyzed reaction under the same conditions.

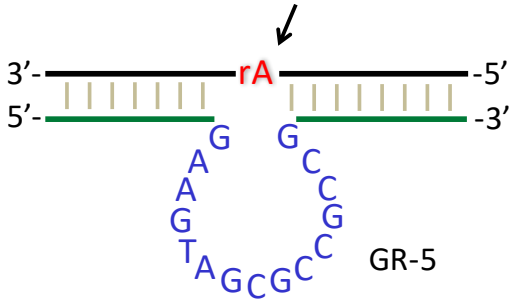

Figure 1.2 The catalytic motif of the GR-5 DNAzyme with the cleavage site pointed by the arrow. The 15 nucleotides (in blue color) compose the catalytic loop which is responsible for the catalytic activity.

1.2.2 Examples of metal-specific DNAzymes

Similar to protein enzymes and ribozymes, DNAzymes require specific metal ions as cofactors to catalyze chemical reactions. In other words, DNAzymes show high selectivity towards respective metal ions, and their catalytic activity may highly dependent on metal ion concentrations. For instance, the 10-23 DNAzyme was isolated through *in vitro* selection under simulated biological conditions (150 mM KCl, 2 mM $MgCl_2$, 50 mM Tris buffer, pH 7.5, 37℃).[11] As shown in Figure 1.3A, its catalytic domain is composed of 15 nucleotides. The catalytic activity of the 10-23 DNAzyme is Mg^{2+}-dependent with a rate of ~0.1 min^{-1} in the

presence of 2 mM Mg^{2+}. By changing the substrate-binding domain, this DNAzyme can be used to target various RNA substrates.

In the meantime, the other DNAzyme, 8-17, was also isolated from the same selection procedure (Figure 1.3B).[11] This enzyme has a relatively small catalytic core, which contains a stem-loop of 3 base pairs and an unpaired loop of 4-5 nucleotides. Unlike the 10-23 DNAzyme, the 8-17 DNAzyme turned out to be substantially more active with Pb^{2+} than other metal ions. Moderate activity of 8-17 was still observed in the presence of many other divalent ions (e.g., Zn^{2+}, Ca^{2+}, Mg^{2+}, Co^{2+}). As a consequence, this DNAzyme was frequently isolated from other subsequent selections.[12-14]

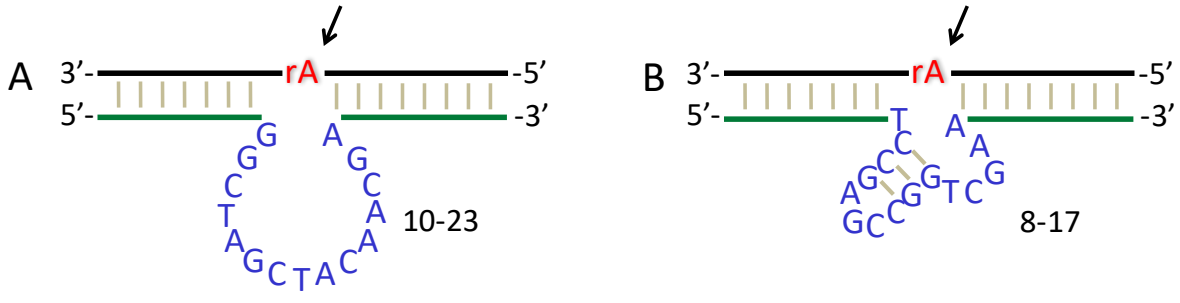

Figure 1.3 Secondary structures of (A) the Mg^{2+}-dependent 10-23 DNAzyme and (B) the Pb^{2+}-dependent 8-17 DNAzyme.

Apart from common metal cofactors in nature, DNAzymes with high activity towards actinide and lanthanide ions were also discovered. For example, a uranyl ion (UO_2^{2+}) -specific DNAzyme called 39E was successfully selected by Liu *et al* (Figure 1.4A).[15] Uranyl salts are toxic and can cause damage to human health when being exposed in the environment. This DNAzyme has $>10^6$-fold higher sensitivity over other competing metal ions. This can be explained by its ultrahigh UO_2^{2+} affinity with a dissociation constant of 97 nM. Subsequent study found that the bulge region might be responsible for UO_2^{2+} binding and catalysis.[16] Its superior

sensitivity and selectivity show potentials in real-time detection and quantification of UO_2^{2+} in the environment.

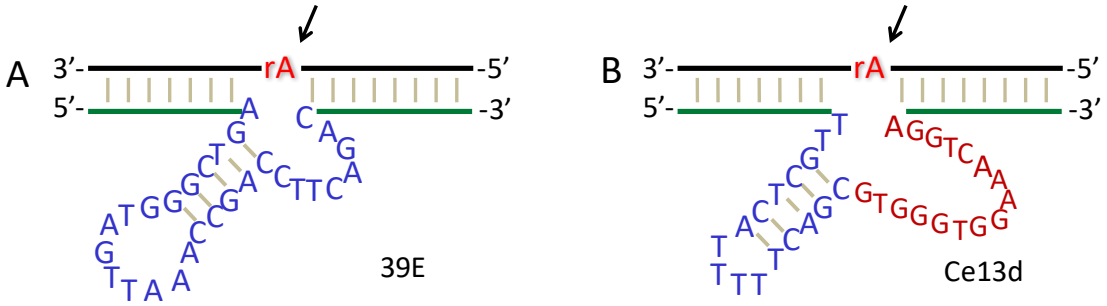

Figure 1.4 Secondary structures of (A) the UO_2^{2+}-dependent 39E DNAzyme and (B) the Ce^{3+}-dependent Ce13d DNAzyme.

Recently, several novel DNAzymes were selected by *in vitro* selection using lanthanide ions (e.g., Ce^{3+}, Pr^{3+}, Lu^{3+}, Ho^{3+}, Er^{3+}, Tm^{3+}).[17-19] Most lanthanides are in the +3 oxidation state carrying high charge densities. For instance, the first lanthanide-dependent DNAzyme was selected by Huang *et al.* using Ce^{4+} as the target metal.[17] As shown in Figure 1.4B, their optimized enzyme loop folded into a bulged-hairpin structure. Surprisingly, activity assays revealed that this DNAzyme (named Ce13d) has high activity with all trivalent lanthanides, but it barely has activity with Ce^{4+}. The Ce13d DNAzyme exhibited a cleavage rate of 0.25 min^{-1} in the presence of 10 μM Ce^{3+}. Their mutation study demonstrated that nucleotides in red color are highly conserved which might be critical for catalysis.

1.2.3 Catalytic mechanism of RNA cleavage

RNA-cleaving DNAzymes cleave at a single ribonucleotide within the substrate strand by promoting nucleophilic attack of the 2′-hydroxyl group to the adjacent phosphodiester bond (Figure 1.5).[20] As a genetic material, the DNA duplex is structurally inflexible. Therefore, the

single-stranded catalytic core is responsible for enzymatic activity that can bind functional groups and form tertiary structures. As mentioned above, most DNAzymes are metal-assisted, and require metal ions (e.g., divalent cations) as cofactors to achieve an appreciable reaction rate.[21-23] Ultimately, the substrate strand splits at the cleavage site, resulting in 2′, 3′-cyclic phosphate and 5′-hydroxyl RNA termini.

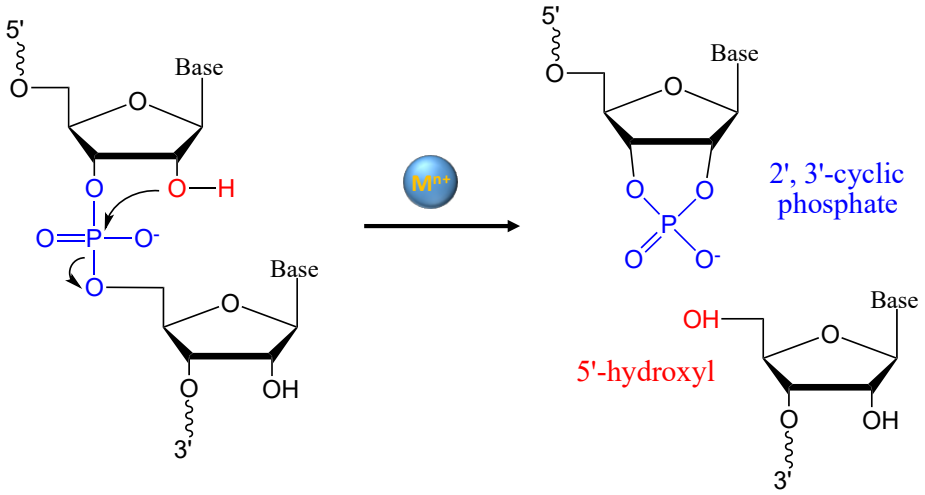

Figure 1.5 Scheme of the RNA cleavage reaction in which the 2′-hydroxyl group attacks the adjacent phosphodiester bond, forming 2′, 3′-cyclic phosphate and 5′-hydroxyl RNA termini. (Adapted from ref. 20)

1.2.4 Role of metal ions in DNAzyme catalysis

Metal ions play critical roles in the DNAzyme catalysis. Many DNAzymes have high binding affinity and specificity toward metal ions. As DNA is a negatively charged polyelectrolyte, DNA folding strongly depends on electrostatics. Therefore, cations may significantly promote the formation of DNAzyme structure.[24] On the other hand, metal ions may serve as catalytic cofactors by directly participating in the chemical reaction.[25] In a RNA cleavage reaction, a metal hydroxide can act as a general base assisting the deprotonation the 2′-

hydroxy group by attracting the proton (Figure 1.6b). Alternatively, a metal ion can function as a Lewis acid to coordinate directly to the 2′-oxygen (Figure 1.6d). In another mechanism, a metal-bound water molecule as a general acid stabilizes the negative charge on the 5′-oxygen (Figure 1.6a), which can also be achieved by direct coordination of a metal ion Lewis acid (Figure 1.6c). Besides, a metal ion as an electrophilic catalyst might make the phosphorus center more reachable for the nucleophilic attack by coordinating with the non-bridging oxygen (Figure 1.6e). As described above, metal ions can facilitate the RNA cleavage reaction through many possible ways. Generally, a metalloenzyme displays an increase in the catalytic rate with an increasing concentration of its cofactors.

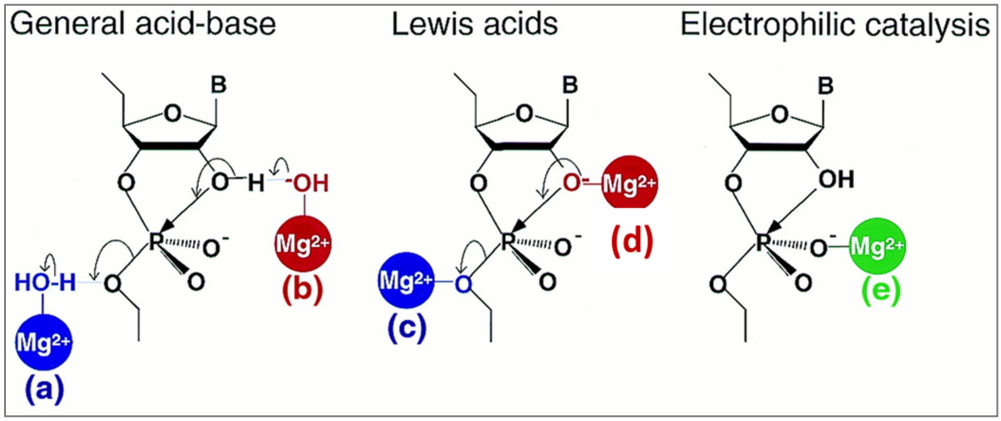

Figure 1.6 Potential catalytic roles of metal ions in the cleavage of a phosphodiester bond. Metal ions can act as (a) a general acid, (b) a general base, (c) a Lewis acid, (d) a Lewis base, and (e) an electrophilic catalyst. (Adapted from ref. 25) Copyright © 2001 Oxford University Press

1.2.5 Applications of DNAzymes

The discovery of artificial DNAzymes significantly expanded the variety of functional nucleic acids for various scientific disciplines, such as biosensing, nanodevices, logic gate operations and material assembly.[26-28] The interest in using DNAzymes as molecular tools for

various applications arises from their inherent superiorities. In contrast to proteins or RNA-based enzymes, DNAzymes are relatively affordable, easily prepared and impressively stable. Generally, the phosphodiester bonds of DNA are almost 1000-fold more resistant to hydrolytic degradation than peptide bonds under physiological conditions as well as 100,000-fold compared to RNA.[9] Also, DNA is available for modification with many fluorophores and other functional groups, or alternatively, conjugation with nanoparticles yielding multifunctional materials.[29]

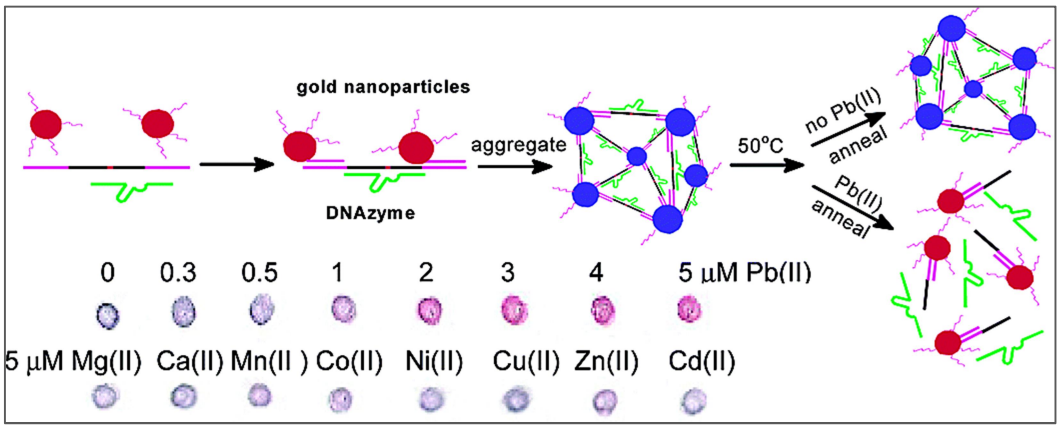

Figure 1.7 A scheme showing a colorimetric Pb^{2+} biosensor using DNAzyme-directed assembly of gold nanoparticles. In the presence of Pb^{2+}, the 8-17 DNAzyme catalyzes the cleavage reaction and disassemble the aggregation leading to a color change from blue to red. The sensor performed colorimetric detection with different Pb^{2+} concentrations and with eight other divalent metal ions. (Adapted from ref. 36) Copyright © 2003 American Chemical Society

Especially, the fact that DNAzymes exhibit nucleic acid cleavage activities in the presence of specific metal cofactors has been elicited to design metal ion biosensors, such as Pb^{2+},[30] Mn^{2+},[31] Mg^{2+},[32] Cu^{2+},[33] Co^{2+},[34] ,UO_2^{2+}.[35] Figure 1.7 describes a remarkable example of a colorimetric lead biosensor based on 8-17 DNAzymes.[36] The biosensor consists of DNA-modified gold nanoparticles, substrates, and DNAzymes. Three components were designed to be able to self-assemble by base pairing. Such self-assembling can lead to the aggregation of gold

nanoparticles and show a blue color. In the presence of Pb^{2+}, the 8-17 DNAzyme catalyzes the cleavage reaction and disassemble the aggregation leading to a red color. The DNAzyme-gold nanoparticles sensor exhibits high sensitivity and selectivity toward Pb^{2+}.

1.3 *In vitro* selection of DNAzymes

In vitro selection or SELEX (systematic evolution of ligands by exponential enrichment) aims to isolate the functional nucleic acids from large random-sequence pools. Since 1990, this methodology has been used to identify DNA or RNA sequences (aptamers) with specific binding affinities for small biomolecules.[37] The successful isolation of the nucleic acid ligands has shown potential in therapeutic and diagnostic applications.[38-39] *In vitro* selection is also applicable to artificial ribozymes catalyzing a growing variety of chemical reactions, such as RNA cleavage,[40] ligation,[41] alkylation,[42] and phosphorylation.[43] To date, all known DNAzymes were isolated through *in vitro* selection. Since the first report in 1994, many methods have been developed to optimize the selection experiments based on different DNA-catalyzed reactions.[44] However, the basic principles of reaction, separation, and amplification are consistent between the different selection strategies.

Here, the *in vitro* selection process of RNA-cleaving DNAzymes is described; this is currently the most thoroughly studied research topic (Figure 1.8).[45] The selection experiment begins with a large population of DNA molecules (~10^{14}) with a 40-80 nucleotide random region and two constant regions. In most cases, a RNA phosphodiester bond is around 100,000 fold more facile to hydrolyze compared to DNA.[9] Thus, a sole ribonucleotide (i.e., rA) is embedded in the DNA substrate strand, indicating the cleavage site. The DNA pool is then incubated under suitable buffer conditions to perform RNA cleavage reaction. During this selection step, several parameters are tunable including the concentrations and identities of metal ions, the temperature,

the pH value, and the incubation time. As a consequence, a small number of DNA molecules can successfully catalyze the RNA cleavage reaction.

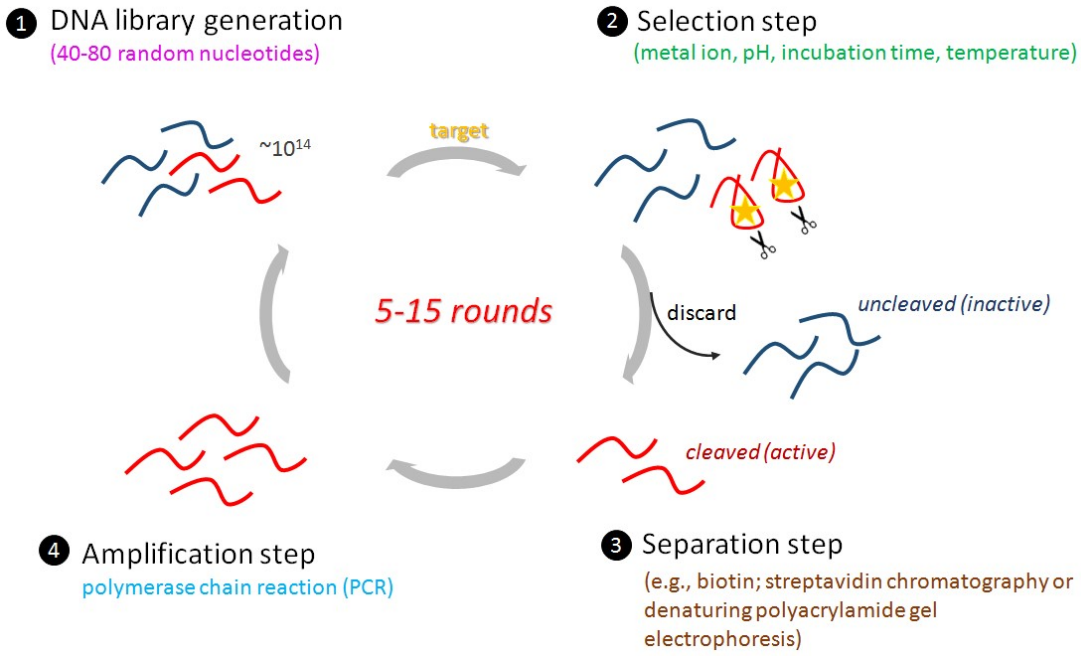

Figure 1.8 *In vitro* selection strategy of RNA-cleaving DNAzymes.

To separate the desired cleaved products from the uncleaved DNA molecules, either biotin; streptavidin chromatography[11,46] or denaturing polyacrylamide gel electrophoresis (dPAGE)[17,47] can be used to achieve the isolation. A biotin moiety attached DNA sequence can be immobilized on a streptavidin column; this only allows the active sequences (cleaved) to flow through. Alternatively, gel-based separation can also detect the size change of DNA molecules due to the cleavage reaction. However, fluorescent modification is always required for the observation and isolation. Afterwards, polymerase chain reaction (PCR) is introduced to amplify the cleaved DNA sequences, as well as regenerate the DNA pool which is ready for the next round of selection. To enrich the DNA pool of catalytically active sequences, the above procedures can be repeated for multiple rounds (5-15 rounds) until the activity becomes

sufficiently high. At the end of the selection, individual sequences in the pool will be cloned and identified. In addition, negative selection steps can be performed to increase the metal specificity by excluding the sequences that are active with competing metal ions.[48]

1.4 Cobalt(III) hexammine

Cobalt is a transition metal element with an atomic number of 27. Common oxidation states of cobalt are +2 and +3. As one of its most important coordination complexes, cobalt(III) hexammine [$Co(NH_3)_6^{3+}$] consists a central Co^{3+} coordinated by six ammonia orthogonal ligands. As shown in Figure 1.9, $Co(NH_3)_6^{3+}$ has roughly the same ionic radius and geometries of magnesium(II) hexahydrate [$Mg(H_2O)_6^{2+}$].[49]

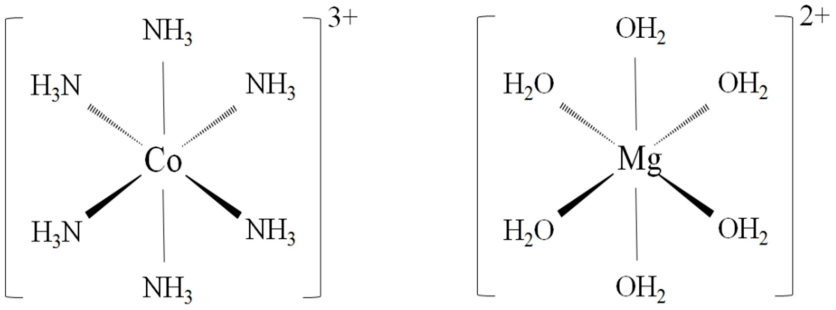

Figure 1.9 Chemical structures of $Co(NH_3)_6^{3+}$ and $Mg(H_2O)_6^{2+}$. The former is exchange-inert while the latter is labile to ligand exchange.

Since the ammonia ligands of $Co(NH_3)_6^{3+}$ are kinetically stable, they do not exchange with solvent to allow inner-sphere interactions with the functional groups in RNA.[50] These properties make $Co(NH_3)_6^{3+}$ a good probe in studying metal-RNA interactions. For example, NMR spectroscopy studies showed that $Co(NH_3)_6^{3+}$ can replace $Mg(H_2O)_6^{2+}$ in outer-sphere coordination and interact with RNA in a similar manner.[49,51-52] In addition, $Co(NH_3)_6^{3+}$ has been used to probe RNA hairpins that contain G-U wobble pairs by electrospray ionization mass

spectrometry (ESI MS).[53] Due to the rigid structure of duplex DNA, limited works have been reported to study the interaction between $Co(NH_3)_6^{3+}$ and DNA. It has been shown that $Co(NH_3)_6^{3+}$ causes DNA condensation by inducing DNA conformation changes.[54] Besides the electrostatic attractions between cations and the negative phosphate group of DNA, major groove binding was also observed for $Co(NH_3)_6^{3+}$.[55] Moreover, $Co(NH_3)_6^{3+}$ was found to be able to bridge the phosphates from opposing strands in the bend across the major groove and stabilize the A-DNA structure.[56]

As noted above, inner-sphere coordination between metal ions and RNA is normally required in RNA cleavage reactions. Due to the tight binding of ammine ligands, $Co(NH_3)_6^{3+}$ does not exchange to allow coordination with phosphate oxygens or with water molecules to generate metal hydroxides.[50] As a consequence, the competition from exchange-inert $Co(NH_3)_6^{3+}$ may provide insights into the metal-RNA interactions required for ribozyme catalysis.[57-59] DeRose and co-workers have reported that the addition of $Co(NH_3)_6^{3+}$ induced Mn^{2+} displacement and inhibition of a hammerhead ribozyme.[60] Based on circular dichroism (CD) and thermal denaturation results, a specific binding affinity of $Co(NH_3)_6^{3+}$ appeared to be responsible for the inhibition effect by inducing structural changes. They ultimately concluded that at least two metal sites support hammerhead activity, one of which requires inner-sphere interactions. In contrast, the addition of $Co(NH_3)_6^{3+}$ was found to promote the Mg^{2+}-induced self-cleavage of the *Neurospora* VS ribozyme.[61] Despite that $Co(NH_3)_6^{3+}$ alone failed to induce self-cleavage, $Co(NH_3)_6^{3+}$ assists the folding of the VS ribozyme in the presence of Mg^{2+}. In the hairpin ribozymes, $Co(NH_3)_6^{3+}$ alone can support efficient activity without additional divalent ions.[62] The study demonstrated that the rate-determining step in hairpin cleavage may not depend on direct coordination to phosphate oxygens or metal-bound hydroxide.

Recently, a similar competition method has been applied to investigate the role of metal ions in RNA-cleaving DNAzymes. Titration with $Co(NH_3)_6^{3+}$ inhibited the activity of an *in vitro* selected, bipartite DNAzyme.[63] This indicated that there was at least one outer-sphere metal-binding site on the DNAzyme.

1.5 Research focus

The initial goal of this research is to select DNAzymes that require $Co(NH_3)_6^{3+}$ as a metal cofactor through *in vitro* selection. Since $Co(NH_3)_6^{3+}$ is exchange-inert, DNAzymes obtained from the selection was expected to exclusively use outer-sphere mechanism for cleavage. The *in vitro* selection, however, resulted in active sequences that are independent of $Co(NH_3)_6^{3+}$, but instead, dependent on Na^+. A detailed analysis of these sequences was performed revealing a new mutant of a previously reported Na^+-specific DNAzyme. A series activity assays were carried out to characterize the catalytic activity of this new mutant. In the meantime, a thorough comparison between NaA43 and this mutant was included focusing on their structures and catalysis. In addition, a preliminary application was explored by converting the new mutant into a folding-based Na^+ sensor using 2-aminopurine (2AP) as fluorescent probes.

Chapter 2. DNAzyme selection with $Co(NH_3)_6^{3+}$

2.1 *In vitro* selection experiment

The experiment of *in vitro* selection followed an established protocol in our lab with a few minor modifications.[17-18] This *in vitro* selection was carried out with an initial library containing approximately 10^{14} random DNA sequences. Briefly, the initial DNA library was prepared by ligating two pieces of DNA (Lib-FAM and Lib-rA). Each DNA sequence contains a 50-nucleotide random region flanked by two short binding arms (Figure 2.1A). This size is chosen as a balance of complexity, diversity, and sequence space coverage. The rA linkage embedded in the binding arm represents the putative cleavage site.

As the intended target, hexaamminecobalt(III) chloride [$Co(NH_3)_6Cl_3$] was used to induce the cleavage reaction due to its good solubility and stability.[64] After incubating the initial library with 10 μM $Co(NH_3)_6Cl_3$ for 1 h, the reaction was quenched by 8 M urea (Step 1). Due to the uncertainty of the optimal pH, two separate selections were carried out independently in this work. The reaction was performed under either pH 6 or pH 7.5 with other conditions remaining identical. It is noteworthy that 1 mM ethylenediaminetetraacetic acid (EDTA) was added in the selection buffer to chelate any possible competitive cations (i.e., Ca^{2+}, Fe^{3+}, Zn^{2+}). EDTA is a versatile chelating agent that can form four or six coordination bonds with a metal ion to prevent its interference.[65] Ideally, a small fraction of DNA sequences can fold into a proper structure in the presence of $Co(NH_3)_6^{3+}$, and cleave at the RNA junction. As shown in Figure 2.1B, the cleaved sequences (91 nt) was then be separated from the uncleaved full-length DNA (119 nt) in 10% dPAGE (Step 2).

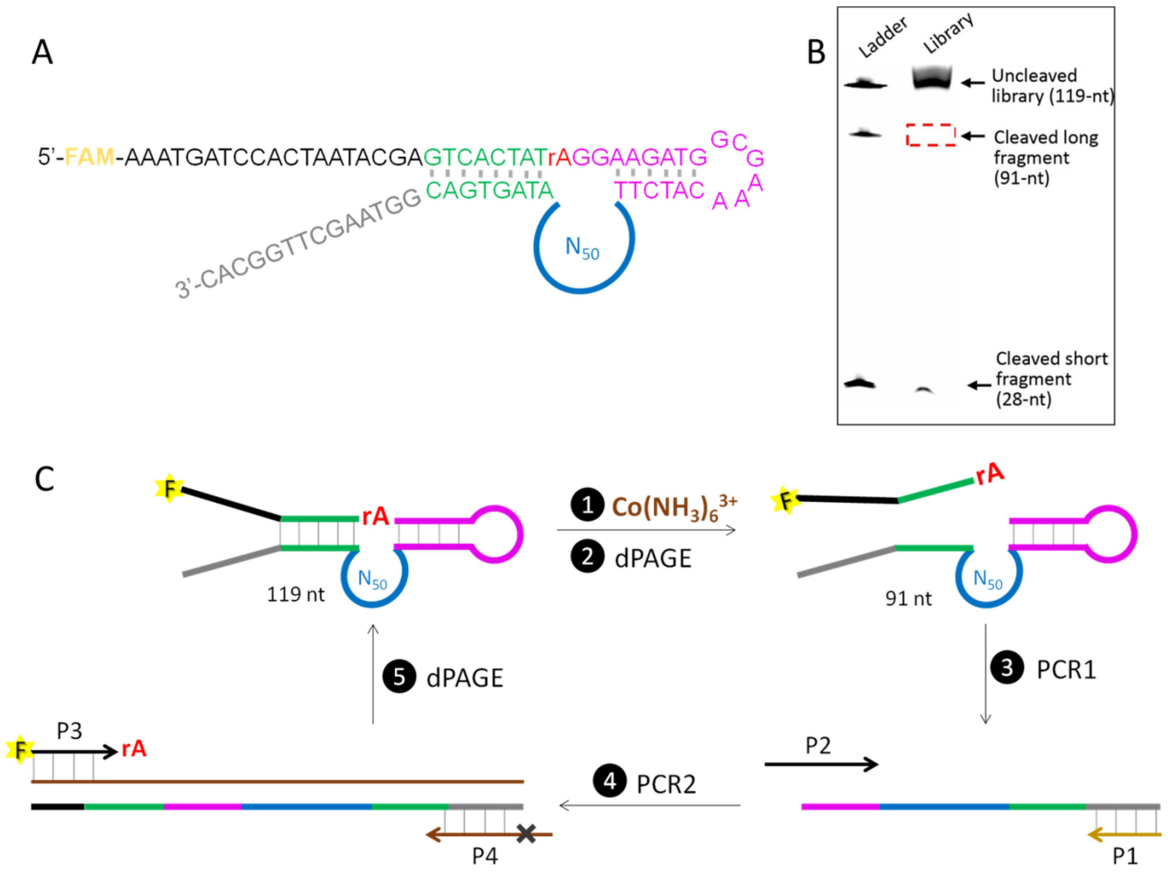

Figure 2.1 (A) The sequence of the initial library containing N_{50} randomized region with a fluorophore labeled at the 5′ end. (B) An example of using 10% dPAGE gel to separate cleaved sequences (91-nt) from uncleaved library (119-nt) by referring to DNA ladder. (C) A designed scheme for the $Co(NH_3)_6^{3+}$ DNAzymes selection involving five main steps. The two rounds of PCR are to amplify the cleaved DNA sequences, and the dPAGE in step 5 is to isolate the positive strand after PCR.

After each selection step, two rounds of PCR were performed to amplify the cleaved DNA sequences (Figure 2.1C). In PCR1, the cleaved sequences were extended and amplified to generate full-length templates for PCR2 (Step 3). Meantime, agarose gel electrophoresis was applied to monitor the amplification progress of PCR1. In PCR2, two functionally modified primers were used to complete the regeneration of DNA library (Step 4). P3 primer contains a 6-carboxyfluorescein fluorophore (FAM) on its 5′-end terminus and a rA base on its 3′-end

terminus. And P4 primer contains a polymer spacer that can stop the polymerase reaction. After gel electrophoresis, the positive strand which contains both FAM and rA was isolated for the subsequent selection round (Step 5). Ideally, 5 to 15 rounds of selection are able to harvest the active sequence in the DNA library.

2.2 Results and discussion

Throughout this selection, the concentration of $Co(NH_3)_6Cl_3$ remained as 10 μM, and the incubation time was always 1 h. Due to the FAM label, the cleavage yield of each selection can be monitored by the fluorescence ratio between the uncleaved library and the cleaved fragment [$\text{Cleavage\%} = \frac{Cleaved\ short\ fragment\ (28\ nt)}{Uncleaved\ \ library\ (119\ nt)}$]. The progressions of selection are summarized in Figure 2.2 showing the cleavage yield of each round. For pH 7.5, the cleavage% slightly increased during the first 4 rounds (black bars). However, the library failed to maintain its activity in the rest of rounds. For pH 6, a gradual increase in the cleavage activity was observed (red bars). At round 6, ~24% of the library was cleaved indicating that active sequences dominated the library as hypothesized. We decided to stop the selection here and carried out one round of negative selection for pH 6. In the negative selection, the library regenerated from the round 6 was incubated in the selection buffer only without the addition of $Co(NH_3)_6^{3+}$. After 1 h of incubation, a 12% cleavage was observed which indicates the nonspecific cleavage (blue bar). To identify the selected sequences, we sent the library sample of round 6 for deep sequencing.

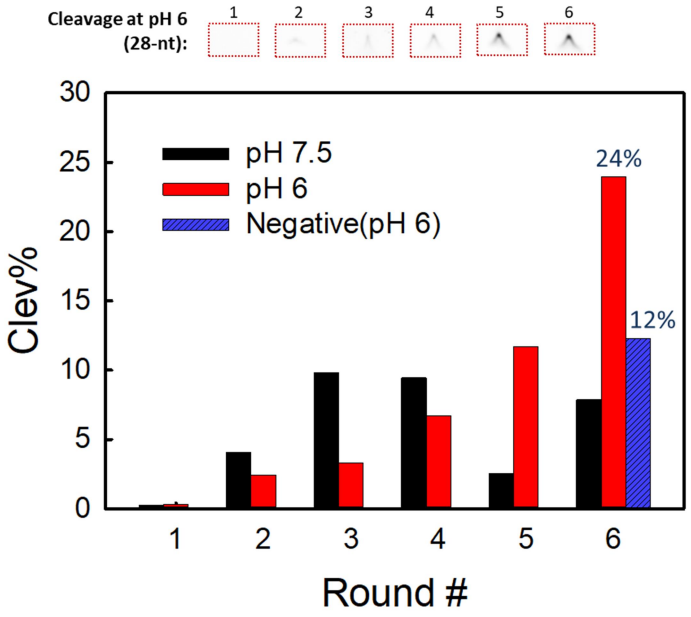

Figure 2.2 Progress of the *in vitro* selection at pH 7.5 or pH 6 showing the cleavage% of each round. For the pH 6 selection, the gradual increase observed in gel images was shown at the top.

2.3 Sequencing analysis

The deep sequencing result included a total of 97,533 sequences. After the sequencing alignment (Geneious®8.1.7), 21,919 reads were successfully assembled into 1,000 families. The most populated first 200 families account for around 50% of the analyzed sequences. Interestingly, more than half of the first 100 families contain almost identical sequences with few differences at some fixed locations. For example, Table 1 listed main sequences of the top 20 most populated families in the selected library. Among them, 19 families are homogeneous which all contain a motif of AGGTCAAAGGTGGGTG (purple colored) in the N_{50} region. This motif is known to be critical for the cleavage activity of the known lanthanide-dependent DNAzyme, Ce13d. The major difference between these families lies in one nucleotide (red colored), which locates at the end of the N_{50} region. Statistically, the possibility of the base being T is about 53% within these 20 families, while 47% of the sequences have an A at this site. Due

to their huge population in the library, this sequence category is likely to be responsible for the cleavage activity observed during the selection experiment. To confirm this hypothesis, it is necessary to verify whether these sequences can fold into a typical DNAzyme structure.

Family #	Sequence (5′---N50---3′)	# copies
1	AAACATCAT-----GGAGCCATAGGTCAAAGGTGGGTGTGGTCGTATCATATCGACCAGCAWT-----AGTGACGG	84
2	AAACATCAT-----GGAGCCATAGGTCAAAGGTGGGTGTGGTCGTATCATATCGACCAGCAWT-----AGTGACGG	81
3	AAACATCAT-----GGAGCCATAGGTCAAAGGTGGGTGTGGTCGTATCATATCGACCAGCAAT-----AGTGACGG	56
4	AAACATCAT-----GGAGCCATAGGTCAAAGGTGGGTGTGGTCGTATCATATCGACCAGCATT-----AGTGACGG	49
5	AAACATCAT-----GGAGCCATAGGTCAAAGGTGGGTGTGGTCGTATCATATCGACCAGCAAT-----AGTGACGG	46
6	AAACATCAT-----GGAGCCATAGGTCAAAGGTGGGTGTGGTCGTATCATATCGACCAGCAWT-----AGTGACGG	44
7	AAACATCAT-----GGAGCCATAGGTCAAAGGTGGGTGTGGTCGTATCATATCGACCAGCAWT-----AGTGACGG	43
8	AAACATCAT-----GGAGCCATAGGTCAAAGGTGGGTGTGGTCGTATCATATCGACCAGCATT-----AGTGACGG	41
9	AAACATCAT-----GGAGCCATAGGTCAAAGGTGGGTGTGGTCGTATCATATCGACCAGCATT-----AGTGACGG	39
10	AAACAT-------GGAGCCATAGGTCAAAGGTGGGTGAGAGTCGTATCATAACGACTCGCAAT-----AGTGACGG	38
11	AAACATCAT-----GGAGCCATAGGTCAAAGGTGGGTGTGGTCGTATCATATCGACCAGCAWT-----AGTGACGG	38
12	AAACATCAT-----GGAGCCATAGGTCAAAGGTGGGTGTGGTCGTATCATATCGACCAGCAWT-----AGTGACGG	38
13	AAACAT-------GGAGCCATAGGTCAAAGGTGGGTGAGAGTCGTATCATAACGACTCGCAAT-----AGTGACGG	36
14	AAACATCAT-----GGAGCCATAGGTCAAAGGTGGGTGTGGTCGTATCATATCGACCAGCAWT-----AGTGACGG	35
15	AAACATCAT-----GGAGCCATAGGTCAAAGGTGGGTGTGGTCGTATCATATCGACCAGCATT-----AGTGACGG	34
16	AAACATCTT-----AGAGGCTTGCAATAAGCTGAGGGATTGAGCATGCGAGGAGTGGTAGTGGAT-----AGTGACGG	32
17	AAACATCAT-----GGAGCCATAGGTCAAAGGTGGGTGTGGTCGTATCATATCGACCAGCAAT-----AGTGACGG	32
18	AAACAT--------GGAGCCATAGGTCAAAGGTGGGTGTGGTCGTATAATATCGACCAGCATT-----AGTGACGG	30
19	AAACATCAT-----GGAGCCATAGGTCAAAGGTGGGTGTGGTCGTATCATATCGACCAGCATT-----AGTGACGG	28
20	AAACATTAT-----GGAGCCATAGGTCAAAGGTGGGTGTGGTCGTATCATATCGACCAGCATT-----AGTGACGG	28

Table 1. Sequences of the top most populated families appeared in the selected library from 5′ to 3′ with the N_{50} random regions in the middle. Among them, 19 families showed a striking similarity in their sequences except the 16th family (grey colored). A homogeneous motif of 16 nucleotides (purple colored) was found in 19 families. The nucleotide varies most frequently among the 20 families was highlighted in

red color. W represents either A or T.

2.4 Secondary structure prediction

In this work, Mfold software was used for secondary structure prediction.[66-67] First, one of the representative sequence (5′-GTC ACT ATA GGA AGA TGG CGA AAC ATC ATG GAG CCA TAG GTC AAA GGT GGG TGT GGT CGT ATC ATA TCG ACC AGC ATT AGT GAC) named CoH1 was folded. Figure 2.3A shows the predicted structure of CoH1 with a red arrow pointing to the cleavage site. This cis-cleaving version of this DNAzyme candidate was further replotted into Figure 2.3B.

Compared to the initial DNA library (Figure 2.1A), a TCTT motif in the binding domain evolved to TCAT (yellow colored) during the selection process, while part of the random region hybridized with the binding domain instead. The rest of the random region, including a 16-nt loop (in purple box), a hairpin structure (in black box), and a 5-nt motif (in red box), composed its hypothetical catalytic core. Note that the prediction was based on a hypothetical ionic strength of 1 M NaCl, while the actual selection buffer used contains only ~25 mM Na^+. Therefore, the T·G wobble pair and two Watson-Crick base pairs shown above the hairpin structure might not be reliable. In addition, a T in the 5-nt-motif between the wobble pair and the binding arm, may or may not form base pair with an A near the cleavage site. Since the major difference lies in the 5-nt motif, most of those populated sequences fold into a similar secondary structure.

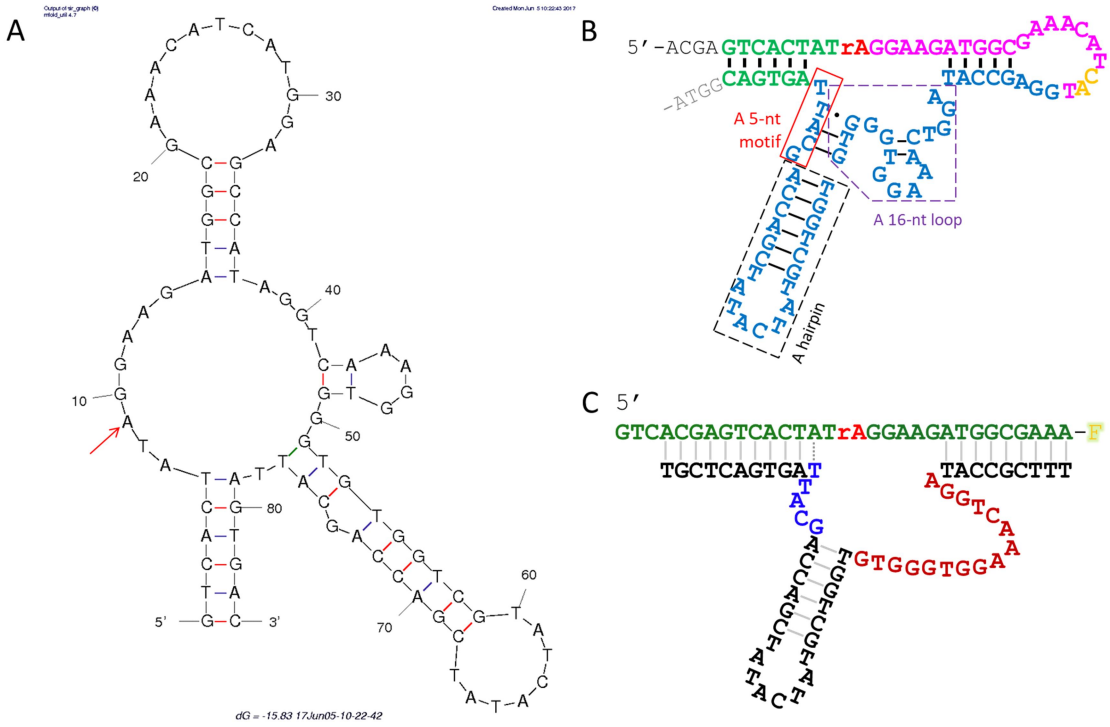

Figure 2.3 (A) Secondary structure predicted by the Mfold software with a red arrow pointing to the RNA site. (B) The cis-cleaving version of CoH1 consists of two duplex regions flanking a hypothetical catalytic loop. The presented catalytic loop consists of a 16-nt loop that is identical to the Ce13d DNAzyme, a hairpin, and a 5-nt motif. (C) The trans-cleaving form of CoH1 including a substrate strand (FAM-labeled) and an enzyme strand.

The DNAzyme can be further converted to its trans-cleaving form (Figure 2.3C), which was used for subsequent activity analysis. The substrate strand containing 30 nucleotides was labeled with a FAM group at the 3′-end. The enzyme strand binds to the substrate strand to form two duplex regions flanking the catalytic loop. To ensure the stable duplex structure, the binding arms were extended by 8 base pairs. Based on the literature review, substrate-binding arms play negligible role in the catalysis of DNAzymes, whose length is adjustable as long as sufficient substrate binding stability is retained.[11,68] The catalytic loop of CoH1 contains 16 nucleotides (red colored) which are identical to the Ce13d DNAzyme (Figure 1.4B) selected by our lab

previously.[17] However, Ce13d is known to be inactive under this selection condition based on our knowledge. On the other hand, the existence of an additional 5-nt motif (blue colored) in CoH1 reminded us of another Na^+-dependent DNAzyme, NaA43, reported by the Lu lab in the University of Illinois recently.[69] A more detailed comparison was discussed in the next chapter.

2.5 Materials and methods

2.5.1 Chemicals

In this *in vitro* selection, all the DNA sequences including the DNA library and PCR primers (Table 2) were purchased from Integrated DNA Technologies (IDT, Coralville, IA). Hexammine cobalt (III) chloride was purchased from Sigma-Aldrich. Tris(Hydroxymethyl)aminomethane (Tris), 2-(N-morpholino)ethanesulfonic acid (MES), 2-[4-(2-hydroxyethyl)piperazin-1-yl]ethanesulfonic acid (HEPES), EDTA, sodium chloride, magnesium chloride hexahydrate were purchased from Mandel Scientific (Guelph, Ontario, Canada). Acrylamide/bisacrylamide 40% solution (29:1), urea, 10x TBE solution, ammonium persulfate (APS), agarose, and ethidium bromide were purchased from Bio Basic Inc. TEMED was purchased from OmniPur. SsoFast EvaGreen supermix was purchased from Bio-Rad. T4-DNA ligase, deoxynucleotide (dNTP) solution mix, Taq DNA polymerase with ThermoPol buffer, 10x gel loading dye, and low molecular weight DNA ladder were purchased from New England Biolabs. All solutions used in this work were prepared with Milli-Q water.

DNA name	Sequences and modifications
Lib-FAM-N50	5'-GGCGAAACATCTTN$_{50}$TAGTGACGGTAAGCTTGGCAC-**FAM**
Lib-rA	5'-AATACGAGTCACTATrAGGAAGAT
Splint	5'-AAGATGTTTCGCCATCTTCCTATAGTCCACCACCA
P1 primer	5'-GTGCCAAGCTTACCG
P2 primer	5'-CTGCAGAATTCTAATACGAGTCACTATAGGAAGATGGCGAAACA
P3 primer	5'-**FAM**-AAATGATCCACTAATACGACTCACTATrAGG
P4 primer	5'-AACAACAACAAC-**iSp18**-GTGCCAAGCTTACCG
P701	5'-CAAGCAGAAGACGGCATACGAGATTCGCCTTAGTGACTGGAGTTC AGACGTGTGCTCTTCCGATCTCTGCAGAATTCTAATACGAGTCAC
P501	5'-AATGATACGGCGACCACCGAGATCTACACTAGATCGCACACTC TTTCCCTACACGACGCTCTTCCGATCTGTGCCAAGCTTACCG

Table 2. List of all the DNA sequences used in this selection experiment.

2.5.2 Selection methods

To prepare the DNA library, Lib-FAM DNA (200 pmol), Lib-rA DNA (300 pmol), and splint DNA (300 pmol) were first mixed in annealing buffer (10 mM Tris-HCl buffer, pH 7.5, 10 mM $MgCl_2$). The mixture was then annealed at 90 °C followed by slow cooling down to room temperature. The ligation reaction followed the T4 ligation protocol provided by New England Biolabs. As prepared DNA library was further purified and extracted from 10% dPAGE (650 V, 1 h). In this work, Bio-Rad ChemiDoc MP imaging system was used to take the gel images and quantify the fluorescence. A gel slice containing the DNA library was crushed and soaked in extraction buffer (1 mM EDTA, 10 mM Tris-HCl, pH 7.0). The further purification was achieved by using a Sep-Pak C18 column (Waters). The extracted DNA library was dried in an Eppendorf Vacufuge at 45 °C overnight.

The DNA library was resuspended in selection buffer A (50 mM MES buffer, pH 6, 25 mM NaCl, 1 mM EDTA) or selection buffer B (50 mM HEPES buffer, pH 7.5, 25 mM NaCl, 1

mM EDTA). For each round of selection, 10 μM of $Co(NH_3)_6Cl_3$ was introduced to induce the cleavage reaction. After 1 h of incubation, 8 M urea was added to quench the reaction. The active sequences with 28 nucleotides missing were then separated from the inactive library using 10% dPAGE. Next, the cleaved strands were extracted and purified to serve as the DNA template for PCR.

2.5.3 PCR

First, a real-time PCR (rt-PCR) was carried out to estimate the amount of selected DNA and the cycles for PCR1. A reaction mixture (20 μL) contains the DNA template (1 μL), P1 and P2 primers (400 nM each), and SsoFast EvaGreen Supermix (10 μL). The thermocycling protocol provided by vendor was followed (95 °C for 30 s, 95 °C for 5 s, and 55 °C for 5 s).

For PCR1, a 50 μL reaction mixture contains the DNA template (2 μL), P1 and P2 primers (200 nM each), dNTP mixture (200 μM), 1 × Taq buffer (5 μL), and Taq DNA polymerase (1.25 units). The cycling protocol used in PCR1 is as follows: 94 °C for 5 min; 94°C for 30 s, 55 °C for 30 s, and 72°C for 30 s. In general, the number of cycles varies from 5 to 20 in each round. The reaction product was mixed with 30% glycerol and quantified with 2% agarose gel (120 V, 50 min). Finally, a gel/PCR DNA fragment extraction kit (IBI Scientific) was applied to purify the PCR1 product.

For PCR2, the one-tenth diluted PCR1 product was used as the template. A 100 μL reaction mixture contains the DNA template (2 μL), P3 and P4 primers (250 nM each), dNTP mixture (200 μM), 1×Taq buffer (10 μL), and Taq DNA polymerase (2.5 units). The reaction was carried out for 12 cycles with the same cycling protocol as PCR1. The PCR2 product was

then purified with ethanol precipitation method and 10% dPAGE. After the purification step, the regenerated library was resuspended in 10 uL of selection buffer for the next round of selection.

2.5.4 Sample preparation for sequencing

The round 6 library was first modified before sending for deep sequencing. PCR1 was performed to generate the full-length library as mentioned above. Next, PCR2 was performed to introduce specific index sequences into the library for the Illumina sequencing technology. Instead of P3 and P4, the forward primer (P701) and the reverse primer (P501) were used with their sequences listed in Table 2. The PCR product was then purified with 2% agarose gel (120 V, 50 min). A gel/PCR DNA fragment extraction kit (IBI Scientific) was used to extract the library from the gel. Finally, the purified DNA sample was eluted in 20 μL of Milli-Q water. The DNA concentration measured with a NanoDrop spectrophotometer was ~10 ng/μL. The sample was shipped to McMaster University for sequencing.

Chapter 3. New mutants of a Na^+-specific DNAzyme

3.1 The Ce13d and NaA43 DNAzymes

3.1.1 Background

Since the first discovery of DNAzymes in 1994, enormous efforts have been put in selecting new catalytic DNA which requires divalent metal ions as cofactors. The main motivation was for biosensor development. Although most previous work focused on divalent metal-dependent DNAzymes, significant recent progress has been made on trivalent metal ions especially lanthanide ions (e.g., Ce^{3+}, Pr^{3+}, Lu^{3+}, Ln^{3+}).[17-19] For example, the Ce13d DNAzyme (Figure 3.2A) selected in our group presents a cleavage rate of ~0.25 min^{-1} with 10 μM Ce^{3+}.[17] Its mutation studies indicated that the enzyme loop (red colored) is critical for the catalysis. Any changes to these nucleotides can completely eliminate the activity. The role of the hairpin is mainly to stabilize the structure which is less important.

Apart from multivalent metals, monovalent metal ions, such as Na^+, is also essential for diverse biochemical processes in animal cells. Sodium is one of the most ubiquitous metal ions in both intracellular and extracellular fluids.[70] In cells, the concentration of Na^+ is important for maintaining transmembrane potential and regulating signal transduction pathways. The intracellular Na^+ concentration is ~10 mM, and the extracellular Na^+ concentration is ~142 mM.[71] Normal serum sodium levels are between approximately 135 to 145 mM. A low serum sodium level might result in a human disease called hyponatremia.[72] As a result, it is important to develop cost-efficient biosensors with high sensitivity and selectivity for Na^+ detection in biological fluids.

RNA-cleaving DNAzymes have been considered as a promising method to detect the intercellular Na^+ concentration due to their metal-dependent activity. So far, limited numbers of DNAzymes were discovered showing Na^+ specificity. The EtNa DNAzyme was selected through an *in vitro* selection using hemin as the initial target.[73] It has the highest cleavage rate of 2.0 h^{-1} with 120 mM NaCl, and a superior Na^+ selectivity over other monovalent ions. However, the EtNa DNAzyme requires organic solvents (e.g., ethanol) to achieve its desired activity which greatly hinder its biological applications. Recently, Torabi *et al.* successfully selected a sodium-specific DNAzyme called NaA43 (Figure 3.1A&B) with 400 mM Na^+.[69] As shown in Figure 3.1C, it possesses a cleavage rate of 0.02 min^{-1} with 10 mM Na^+ in reaction buffer (50 mM Bis-Tris, pH 7.0, 90 mM LiCl). The NaA43 DNAzyme showed an apparent dissociation constant (K_d) of ~39.1 mM when serving as a fluorescent Na^+ sensor.

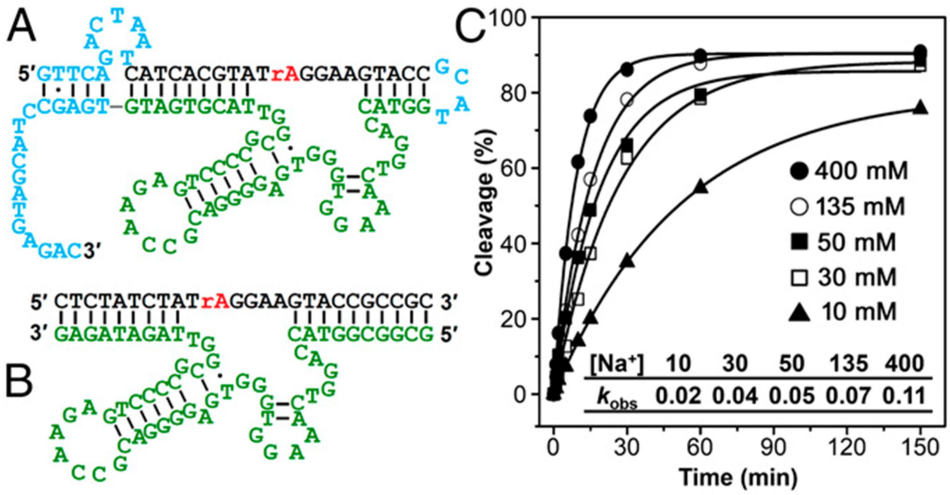

Figure 3.1 Secondary structure of (A) the cis-cleaving and (B) the trans-cleaving NaA43 DNAzymes. (C) The cleavage percentage of the cis-cleaving NaA43 DNAzyme with different concentrations of Na^+ as a function of the incubation time. Inset: cleavage rate or k_{obs} (min^{-1}) of the NaA43 DNAzyme. (Adapted from ref. 69) Copyright © 2015 National Academy of Sciences

3.1.2 Structure comparison

Comparing the Ce13d and NaA43 DNAzymes side by side (Figure 3.2A&B), they both present an identical 16-nucleotide loop (red colored) and a hairpin structure. The rest a few nucleotides marked in blue are their main distinctions. Noting that this similarity is more than a coincident, several systematic studies were published to address this issue.[74-75] First, Torabi and Lu found that the activity of Ce13d requires Na^+ and trivalent lanthanide ions simultaneously.[75] The Na^+-dependent activity of Ce13d was also reported by Zhou *et al.*[74] Since NaA43 uses Na^+ as its sole cofactor, the small motif of TGGCG (blue colored in Figure 3.2B) was believed to replace the role of Ce^{3+} in the reaction. A series of rational mutation studies were carried out by Zhou *et al*. Indeed, they concluded that the G_{23} in this motif as indicated in Figure 3.2B, is critical for the activity of NaA43. Based on their results, the 16-nucleotide loop serves as a conserved Na^+ binding site (Figure 3.2D) which appears in both of the DNAzymes, and the small motif on the left side of the hairpin also plays an important role in the catalysis.

As mentioned above, the predicted structure of CoH1 (Figure 3.2C) is also similar to Ce13d and NaA43. The presence of a 16-nucleotide loop suggests that this DNAzyme candidate may bind to Na^+. Besides, it also has a 5-nt motif on the left side of the hairpin with merely two nucleotides (in red box) differing from NaA43. Taken together, we suspect that this DNAzyme candidate has the Na^+-dependent activity. Since the selection buffer used in our selection contained ~25 mM Na^+, it is possible that the Na^+-active sequences survived from each round. On the other hand, the presence of 1 mM EDTA in our selection helped to eliminate any interference from other multivalent ions but not Na^+. This result also explained the 12% non-specific cleavage observed in the negative selection.

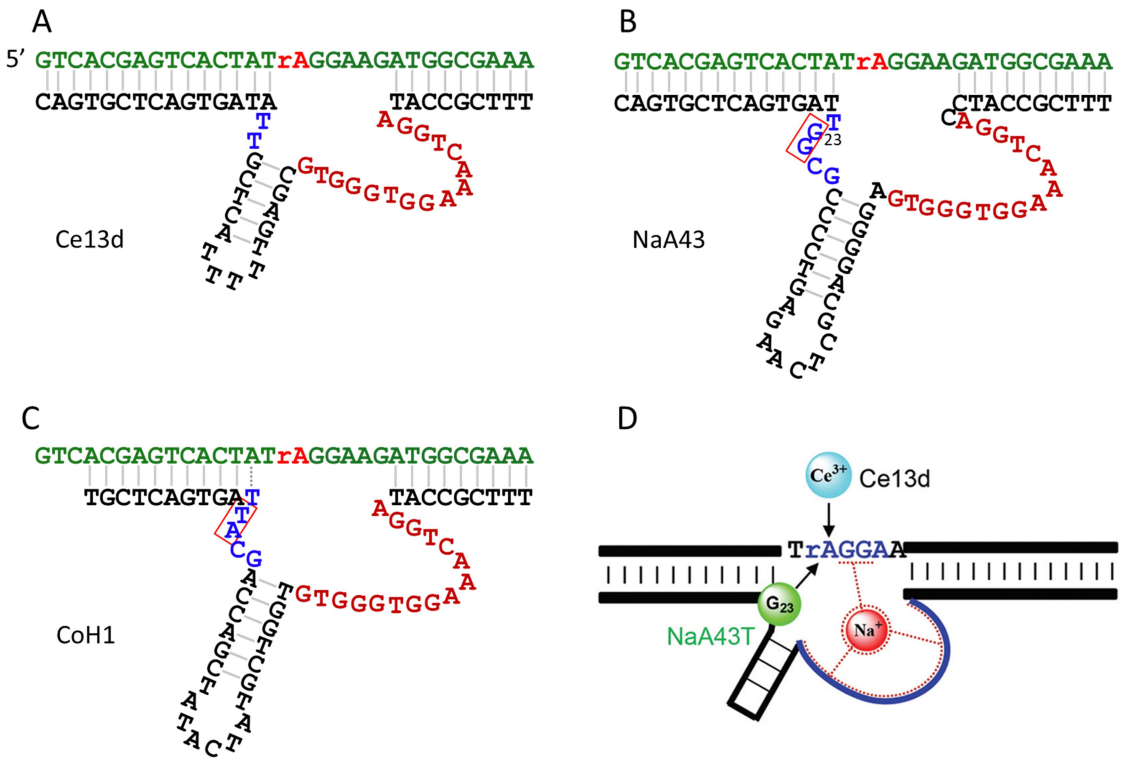

Figure 3.2 The secondary structure of the (A) Ce13d, (B) NaA43, and (C) CoH1 DNAzymes. The identical nucleotides in enzyme loop regions were marked in red color. A nucleotide, G_{23}, was highlighted in the NaA43 DNAzyme. (D) A scheme describing the metal binding sites of Ce13d and NaA43. The enzyme loop and the substrate junction form a selective Na^{+}-binding pocket. In Ce13d, Ce^{3+} binds to the non-bridging oxygen which is replaced by G_{23} in NaA43T. (Adapted from ref. 74) Copyright © 2015 Oxford University Press

Although $Co(NH_3)_6^{3+}$-dependent activity was not achieved, the high activity of the selected sequence attracted our interest. This sequence is similar to the previous NaA43 DNAzyme despite the fact that they were selected from different libraries in distinct selection buffers. In other words, CoH1 can be considered as a mutant of the NaA43 DNAzyme. Based on the previous study, G_{23} in the 5-nt motif is critical for the activity of NaA43.[74] On the contrary, CoH1 presents a T at this site which may result in a different catalytic performance in the reaction. Besides, it is important to further verify the role of this 5-nt motif in RNA cleavage

reaction. Taken these together, mutation studies were designed regarding to 3 nucleotides, $T_2A_3G_5$, in this motif as shown in Figure 3.3. Most of these mutants existed in the selected library with a small population. For each mutant, all of the other parts are identical to the CoH1 except those highlighted nucleotides in the pink box. Currently, a total of 12 sequences were tested as the enzyme strands in the following activity assays.

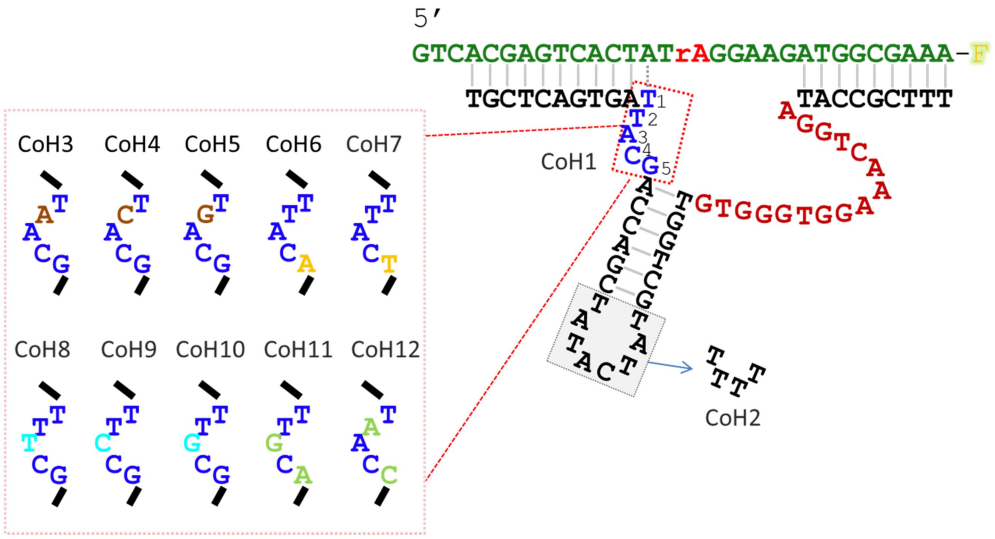

Figure 3.3 Secondary structures of designed mutations based on CoH1. For CoH2, those nucleotides in the shaded box were replaced with TTTT. For CoH3-12, the 5 nucleotides in the red box were replaced with corresponding sequences in the pink box, respectively. Each mutant differs from CoH1 only at those highlighted regions.

3.2 Na^+-dependent activity

To confirm the Na^+-dependent activity, all 12 potential sequences in Figure 3.3 were tested respectively by hybridizing with the FAM-labeled substrate. Each DNAzyme complex was annealed in 50 mM MES buffer (pH 6, pH adjusted using LiOH) containing 25 mM LiCl to prevent background cleavage and to stabilize the duplex regions. The cleavage reaction was carried out in the presence of 20 mM Na^+ at pH 6, which is similar to the selection condition. As

shown in gel images (Figure 3.4B), significant cleavage was observed for CoH1 and CoH2 after 1 h of incubation. The cleavage yields of 12 sequences were analyzed and summarized in Figure 3.4A. Among all the sequences, CoH1 containing the $T_2A_3G_5$ in its 5-nt motif showed the highest cleavage of 45%. This is not surprising since this sequence dominated the selected library. Besides, the high cleavage of CoH2 indicates that the replacement of the loop in the grey box (Figure 3.3) with TTTT does not affect the activity.

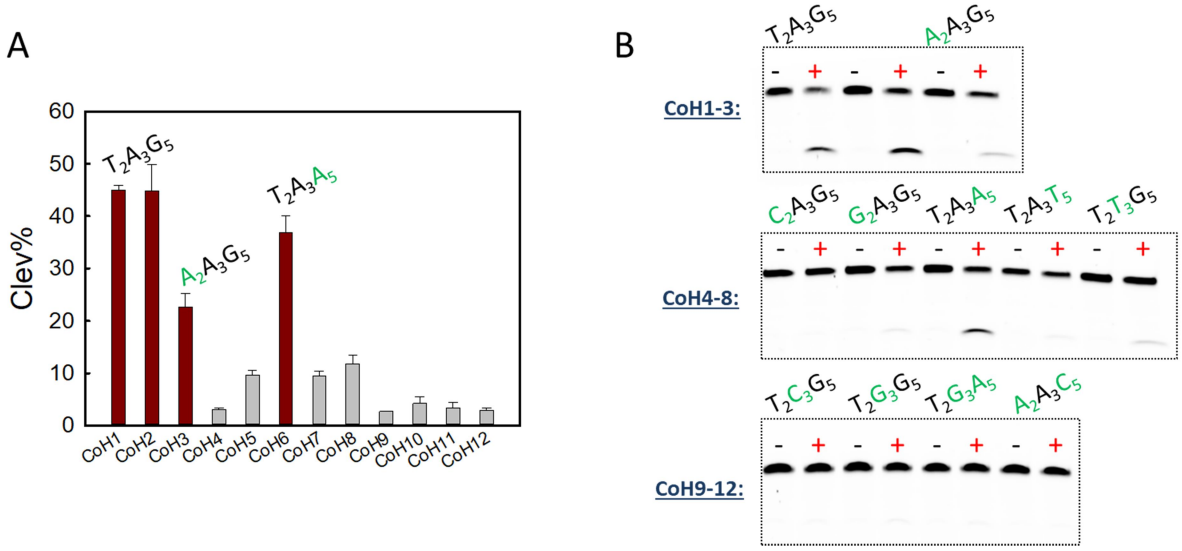

Figure 3.4 (A) Cleavage yield of all 12 sequences in the presence of 20 mM Na^+ for 1 h. (B) Gel images of the Na^+-dependent activity test with the mutations showing above. The upper band represents the uncleaved substrate and the lower band represents the cleaved FAM bearing fragment. For each mutant, the left lane represents the cleavage without Na^+, and the right lane represents the cleavage with 20 mM Na^+ added.

As for other mutants regarding to the $T_2A_3G_5$ nucleotides, CoH6 and CoH3 also exerted moderate activities under such reaction condition. Comparing CoH1, CoH3, CoH4, and CoH5, we found that T_2 is critical for the activity. Mutating this thymine to adenine maintained half of the cleavage activity, while mutating to C or G abolished the activity. Referring to the

sequencing analysis, this activity result explained the fact that this nucleotide appeared to be either T or A in the library. Besides, A_3 turned out to be immutable which failed to tolerate any mutations (CoH8-10). The cleavage activity greatly dropped when replacing G_5 with T_5 (CoH7). However, the G_5 to A_5 mutation is tolerable according to the significant cleavage of CoH6 with only 10% decrease. Since CoH1 with the $T_2A_3G_5$ provided the highest cleavage, it was used for following studies.

The Na^+-dependent activity of CoH1 was further studied by incubating with various concentrations of Na^+. As shown in the gel image (Figure 3.5B), the cleavage% increased with the Na^+ concentration increasing. Quantified cleavage activity was plotted as a function of Na^+ concentration in Figure 3.5A. Below around 1.5 mM, the cleavage activity of CoH1 is linearly related to Na^+ concentration (inset). The cleavage reached the saturation stage in the presence of ~10 mM Na^+. The high cleavage at low Na^+ concentrations suggests a high sensitivity of CoH1 toward Na^+, which may benefit the Na^+ detection in future applications. This is an important advantage considering that the intracellular Na^+ concentration is only around 10 mM.

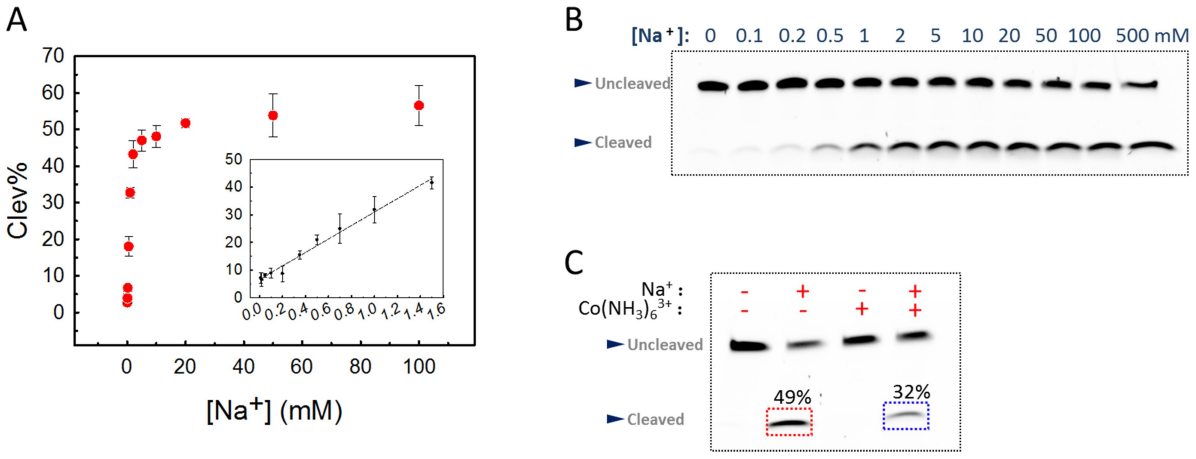

Figure 3.5 (A) Cleavage yield of CoH1with various Na^+ concentrations in 1 h. Inset: the linear response region with [Na^+] below 1.5 mM. (B) A gel image showing the cleavage with [Na^+] ranging from 0 to 500

mM. The upper band represents the uncleaved substrate and the lower band represents the cleaved FAM bearing fragment. (C) The inhibition effect of $Co(NH_3)_6^{3+}$ (10 μM) on the cleavage activity of CoH1.

Since $Co(NH_3)_6^{3+}$ was used as the intended cofactor during the selection, it is necessary to verify its effect on CoH1. As shown in Figure 3.5C, $Co(NH_3)_6^{3+}$ alone failed to initiate the catalysis. In the presence of Na^+, the addition of $Co(NH_3)_6^{3+}$ inhibited the cleavage by 17% compared to Na^+ alone. However, there was still 32% of activity remained. The $Co(NH_3)_6^{3+}$ concentration used in this assay was 10 μM, which is same as the *in vitro* selection experiment. Therefore, this result suggests that $Co(NH_3)_6^{3+}$ failed to serve as a cofactor for this active sequence during the selection. However, CoH1 still survived from the selection process due to the insufficient inhibition caused by $Co(NH_3)_6^{3+}$.

3.3 Cleavage kinetics

Next, the kinetics study on the cleavage reaction of CoH1 was carried out. With different concentrations of Na^+, the cleavage reaction was quenched after various incubation times. For instance, Figure 3.6B shows the cleavage of CoH1 in the presence of 10 mM Na^+. The cleavage yield observed in the gel image was replotted as a function of Na^+ concentration as shown in Figure 3.6A. Each kinetic profile was further fitted into a first-order equation, $\%P_{cleavage,t} = \%P_{max}(1 - e^{-kt})$. $\%P_{max}$ is the maximum cleavage% at the end of the reaction and k is the cleavage rate. In Figure 3.6B, the reaction rate obtained from the fitting was summarized in a chart. With 100 mM Na^+, a cleavage rate of ~0.10 min^{-1} was reached. With only 10 mM Na^+, CoH1 displayed a cleavage rate of ~0.07 min^{-1}. Compared to the NaA43 DNAzyme reported (Figure 3.1C), the rate of cleavage CoH1 is ~3.5-fold higher under the same Na^+ concentration.

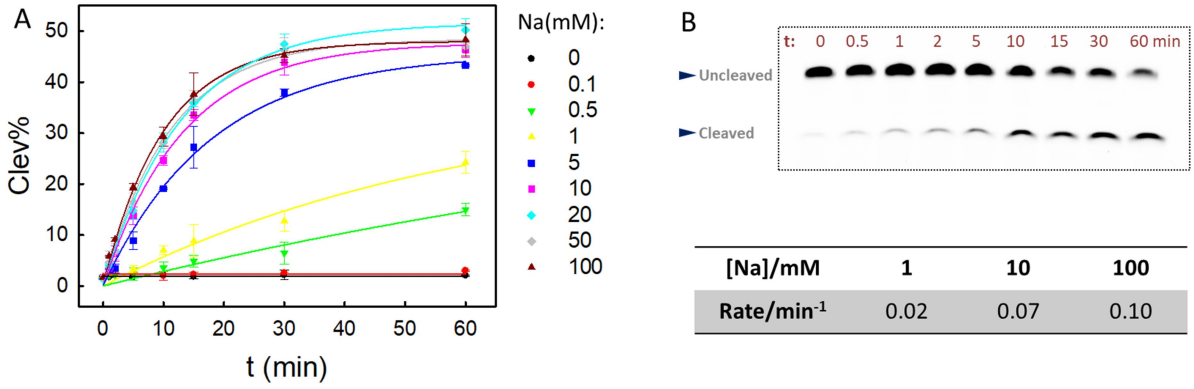

[Na]/mM	1	10	100
Rate/min^{-1}	0.02	0.07	0.10

Figure 3.6 (A) Kinetic profile of the CoH1 DNAzyme with various concentrations of NaCl at pH 6. (B) A gel image showing the kinetics of CoH1 with an incubation time ranging from 0 to 60 min. The upper band represents the uncleaved substrate and the lower band represents the cleaved FAM bearing fragment. The reaction rates obtained from the fitting under various concentrations of Na^+ were summarized in the chart.

Furthermore, we plotted the cleavage rate of CoH1 as a function of Na^+ concentration (Figure 3.7). The cleavage rate increases with a rising concentration of Na^+ and reaches a saturation stage. Its enzyme kinetics was then fitted into a one-site saturation binding curve with an apparent dissociation constant (K_d) of 4.3 ± 0.6 mM Na^+. As described above, NaA43 presented a K_d value of ~39.1 mM when serving as a fluorescent Na^+ sensor. Under its optimal condition (50 mM MES, pH 6, 25 mM LiCl), CoH1 has a stronger Na^+-binding affinity than NaA43.

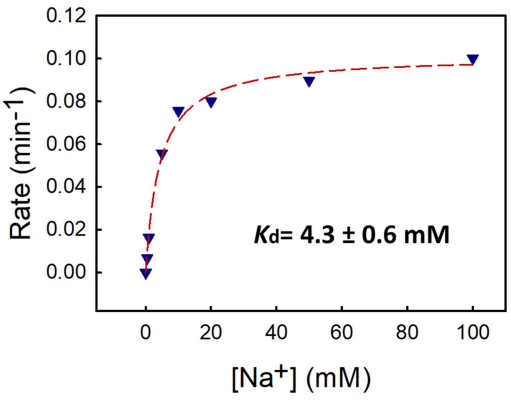

Figure 3.7 The cleavage rate of CoH1 as a function of Na^+ concentration. The one-site binding equation used for fitting is $v = v_{max} \cdot [M^+]/(k_d + [M^+])$, where v is the reaction rate, $[M^+]$ is the Na^+ concentration, and k_d is the apparent dissociation constant.

3.3.1 pH-dependent activity

From structure comparison, we noticed that CoH1 differs from the NaA43 mainly on 2 critical nucleotides (Figure 3.2A&B). However, CoH1 exhibited a higher cleavage rate and superior sensitivity at low Na^+ concentrations in our activity assays. Thus, a more systematic comparison should be made for better understanding these two Na^+-dependent DNAzymes. The optimal reaction condition of NaA43 as reported contains 50 mM Bis-Tris, pH 7, 90 mM LiCl.[69] On the contrary, CoH1 was selected through *in vitro* selection using 50 mM MES buffer, pH 6. As a result, we suspected that the reaction pH might be responsible for the distinct performance of these two DNAzymes. To test this, we compared the kinetics of NaA43 with CoH1 and the other two active mutants (CoH3 and CoH6) at either pH 6 or pH 7. In the presence of 10 mM Na^+, our active sequences (CoH1, CoH3, and CoH6) catalyzed the cleavage reaction with a faster rate under pH 6 (Figure 3.8A). At pH 7, NaA43 performed a higher cleavage activity than CoH1, CoH3, and CoH6 (Figure 3.8B).

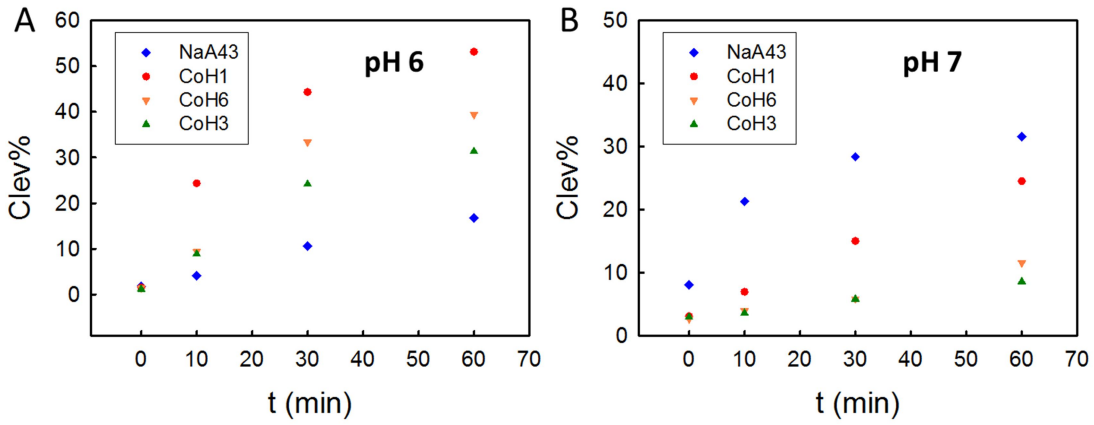

Figure 3.8 The kinetics studies on NaA43 (blue diamond), CoH1 (red circle), CoH3 (green triangle), and CoH6 (yellow triangle) with 10 mM NaCl at (A) pH 6 or (B) pH 7.

Above results indicated that pH is an important parameter to distinguish these two DNAzymes. The pH-dependent assays were performed with the addition of 10 mM Na^+ in various pH buffers. As shown in Figure 3.9A, the activity of CoH1 increased from pH 4.5 to pH 6.0 and decreased at higher pH. The optimal reaction condition of CoH1 turned out to be pH 6.0. By contrast, the highest activity of NaA43 was observed at pH 7.0. Overall, CoH1 performs higher cleavage activity at pH below ~6.5, while NaA43 has more advantages at higher pH. Referring to the structures of these two DNAzymes, it is interesting to note that few mutations in the 5-nt motif resulted in distinct pH-dependent activity. The pKa value of T_2A_3 nucleotides in CoH1 might be responsible for its high activity at low pH. Future efforts could be paid to understand the pH-dependent mutations in more details. Besides, such property indicates the advantages of applying CoH1 for Na^+ detection in relatively acidic environment such as cancer cells.[76]

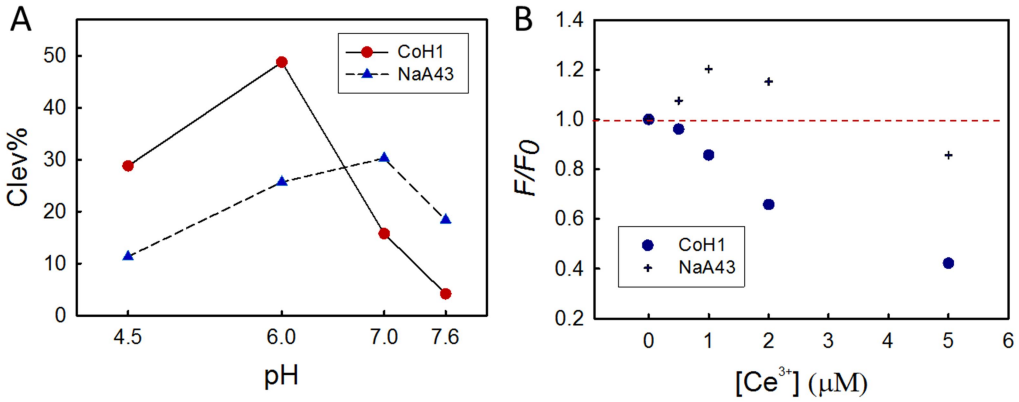

Figure 3.9 (A) Cleavage yield of CoH1 and NaA43 with 10 mM NaCl at different pH for 30 min. (B) The normalized cleavage of CoH1 and NaA43 as a function of Ce^{3+} in the presence of 10 mM NaCl. Dots above the red standard line represent the promotion caused by Ce^{3+}, while those below the red standard line represent the inhibition by Ce^{3+}.

3.3.2 The effect of Ce^{3+}

In previous study, the activity of NaA43 can be accelerated by Ce^{3+}. This was explained by the Ce^{3+}-involved mechanism, in which Ce^{3+} binds to the non-bridging oxygen and neutralizes the evolving negative charge in the transition state.[74] To further understand the cleavage mechanism, the effect of Ce^{3+} was studied for both CoH1 and NaA43 in the presence of 10 mM Na^+ (Figure 3.9B). The y-axis was the ratio of the cleavage with both Na^+ and Ce^{3+} over the cleavage with Na^+ only. In the figure, the area above the red line represents the promotion effect of Ce^{3+}, while the area below represents the inhibition effect. Indeed, low concentrations of Ce^{3+} promoted the catalysis of NaA43 at pH 7. However, the activity of CoH1 decreased linearly with the gradual addition of Ce^{3+}. Unlike NaA43, CoH1 is dominated by Na^+ only with Ce^{3+} playing no positive role in its cleavage activity.

3.4 Metal specificity test

For traditional Na^+ probes, detecting Na^+ with high selectivity over other monovalent ions (e.g., K^+) is still a challenge.[77] To determine the metal specificity of CoH1, a total of 20 metal ions including monovalent, divalent, and trivalent ions were tested at pH 6. In this experiment, concentrations of 10 mM, 1 mM, and 100 μM were used for monovalent, divalent, and trivalent ions, respectively. As shown in Figure 3.10B, CoH1 showed a significant cleavage with Na^+ but not with other monovalent ions tested. Also, none of trivalent ions induced cleavage for CoH1. For divalent ions, a cleavage of ~36% was also observed with 1 mM Pb^{2+} as shown in Figure 3.10A. Many other metal-specific DNAzymes also show activity toward Pb^{2+}, such as Ce13d.[17,73,78] Due to the low concentration of Pb^{2+} in physiological condition, this is not likely to become a concern in future applications. Based on these results, CoH1 displays a high selectivity to Na^+ especially over other competing monovalent ions.

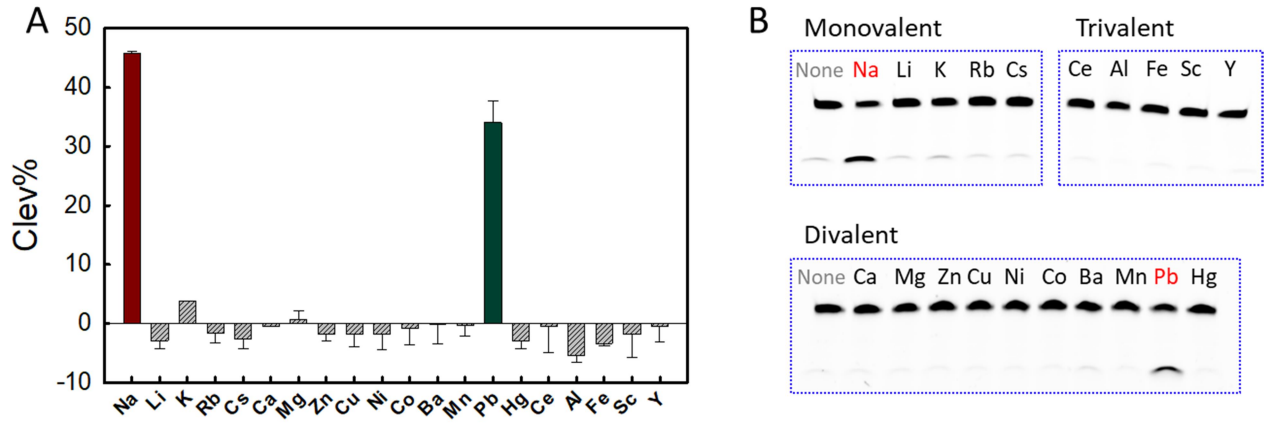

Figure 3.10 (A) Selectivity of CoH1 with 20 different metal ions at pH 6 for 1 h. Each data was normalized by subtracting the background cleavage (without metal). (B) Gel images showing the cleavage in the presence of monovalent (10 mM), divalent (1 mM) and trivalent (100 μM) ions.

3.5 Materials and methods

3.5.1 Chemicals

All the DNA sequences listed in Table 3 were purchased from Eurofins Genomics. NaA43 was purchased from Integrated DNA Technologies (Coralville, IA). Sodium chloride, cesium chloride, calcium chloride dihydrate, magnesium chloride hexahydrate were purchased from Mandel Scientific (Guelph, Ontario, Canada). Other metal salts including lithium chloride hydrate, potassium chloride, rubidium chloride, cerium chloride heptahydrate, scandium chloride hydrate, manganese chloride tetrahydrate, iron chloride hexahydrate, nickel chloride hexahydrate, cobalt chloride hexahydrate, copper chloride dehydrate, zinc chloride, mercury perchlorate, lead acetate, barium chloride dihydrate, aluminium chloride hydrate, yttrium chloride hexahydrate were purchased from Sigma-Aldrich. Sodium acetate, 2-(N-morpholino)ethanesulfonic acid (MES), 2-[4-(2-hydroxyethyl)piperazin-1-yl]ethanesulfonic acid (HEPES) were purchased from Mandel Scientific (Guelph, Ontario, Canada). Lithium hydroxide was purchased from Alfa Aesar. Acrylamide/bisacrylamide 40% solution (29:1), urea, 10x TBE solution, ammonium persulfate (APS) were purchased from Bio Basic Inc. TEMED was purchased from OmniPur. All solutions used in this work were prepared with Milli-Q water. The pH of the buffers was measured with Denver Instrument UltraBasic pH meter.

DNA name	Sequences and modifications
FAM-Sub	5’-GTCACGAGTCACTATrAGGAAGATGGCGAAA-**FAM**
CoH1	5’-TTTCGCCATAGGTCAAAGGTGGGTGTGGTCGTATCATATCGACCAGCATTAGTGACTCGT
CoH2	5’-TTTCGCCATAGGTCAAAGGTGGGTGTGGTCGTTTTCGACCAGCATTAGTGACTCGT
CoH3	5’-TTTCGCCATAGGTCAAAGGTGGGTGTGGTCGTATCATATCGACCAGCAATAGTGACTCGT
CoH4	5’-TTTCGCCATAGGTCAAAGGTGGGTGTGGTCGTATCATATCGACCAGCACTAGTGACTCGT

CoH5	5’-TTTCGCCATAGGTCAAAGGTGGGTGTGGTCGTATCATATCGACCAGCAGTAGTGACTCGT
CoH6	5’-TTTCGCCATAGGTCAAAGGTGGGTGTGGTCGTATCATATCGACCAACATTAGTGACTCGT
CoH7	5’-TTTCGCCATAGGTCAAAGGTGGGTGTGGTCGTATCATATCGACCATCATTAGTGACTCGT
CoH8	5’-TTTCGCCATAGGTCAAAGGTGGGTGTGGTCGTATCATATCGACCAGCTTTAGTGACTCGT
CoH9	5’-TTTCGCCATAGGTCAAAGGTGGGTGTGGTCGTATCATATCGACCAGCCTTAGTGACTCGT
CoH10	5’-TTTCGCCATAGGTCAAAGGTGGGTGTGGTCGTATCATATCGACCAGCGTTAGTGACTCGT
CoH11	5’-TTTCGCCATAGGTCAAAGGTGGGTGTGGTCGTATCATATCGACCAACGTTAGTGACTCGT
CoH12	5’-TTTCGCCATAGGTCAAAGGTGGGTGTGGTCGTATCATATCGACCACCAATAGTGACTCGT
NaA43	5’-TTTCGCCATCCAGGTCAAAGGTGGGTGAGGGGACGCCAAGAGTCCCCGCGGTTAGTGACTCGTGAC

Table 3. List of all the DNA sequences used in above activity assays.

3.5.2 Denaturing polyacrylamide gel electrophoresis (dPAGE)

In this work, denaturing polyacrylamide gel electrophoresis was mainly used to analyze and purify the FAM-labeled oligonucleotides from DNAzyme cleavage reactions. The gel stock solution of 15% dPAGE (500 mL) contains urea (240g), 40% acrylamide (29:1) (187.5 mL), and 10x TBE (50 mL). As a denaturing agent, urea can destroy the secondary structure of DNA which allows DNA separation based on the molecule weight.[79] The gel mixture was prepared by mixing 15% gel stock solution, 10% APS, and TEMED, which was then transferred to the glass plate.

3.5.3 Na^+-dependent activity assays

The FAM-labeled substrate strand was used in all activity assays with sequence showing in Figure 3.3. To form the DNAzyme complex, substrate strands and enzyme strands were first hybridized in buffer A (50 mM HEPES, pH 7, 25 mM LiCl). The pH 7 buffer was used to prevent background cleavage caused by the unexpected Na^+ in water. The DNAzyme complex (2

μM) was prepared by annealing the FAM-substrate (2 μM) and the enzyme (3 μM) in 90°C water, followed by gradual cooling to room temperature. The reaction was carried out in buffer B (50 mM MES, pH 6, 25 mM LiCl). Each reaction had a volume of 7 μL containing DNAzyme complex (200 nM) and 1 μL of NaCl solutions with a concentration gradient (0, 0.1, 0.2, 0.5, 1, 2, 5, 10, 20, 50, 100, 500 mM). After 1 h of incubation, the reaction was quenched with the addition of 8 M Urea (8 μL). The reaction products were separated by 15% dPAGE (200V, for 1 h 20 min) and analyzed by a Bio-Rad ChemiDoc MP imaging system. To test the effect of $Co(NH_3)_6^{3+}$, $Co(NH_3)_6Cl_3$ (10 μM) was introduced into the reaction with or without Na^+ for 1 h.

3.5.4 Kinetics assays

The kinetics assay of CoH1 was carried out in buffer B with different concentrations of NaCl (0, 0.1, 0.5, 1, 5, 10, 20, 50, 100 mM). After various incubation times (0, 0.5, 1, 2, 5, 10, 15, 30, 60 min), the reaction was quenched with the addition of 8 M Urea (8 μL). When comparing the kinetics of CoH1, CoH3, CoH6, and NaA43, reactions were quenched after 0, 10, 30, 60 min, respectively. Buffer C (50 mM HEPES, pH 7, 25 mM LiCl) was used for reactions at pH 7.

3.5.5 pH-dependent and selectivity assays

In pH-dependent assays, CoH1 and NaA43 were incubated with 10 mM NaCl in various pH buffers for 30 min. Acetate buffer (50 mM, with 25 mM LiCl) was used for pH 4.5, and HEPES buffer (50 mM, with 25 mM LiCl) was used for pH 7.6. To test the effect of Ce^{3+}, reactions were performed in the presence of 10 mM NaCl for 1 h. At the same time, 1 μL of $CeCl_3$ stock solution was added to the reaction resulting in a final Ce^{3+} concentration of 0, 0.5, 1, 2, 5 μM. For CoH1, buffer B was used. For NaA43, buffer A was used.

In the selectivity experiment, concentrations of 10 mM, 1 mM, and 100 μM were used for monovalent, divalent, and trivalent ions, respectively. After 1 h, the reaction was quenched and characterized by 15% dPAGE (200V, for 1 h 20 min).

Chapter 4. Na^+ sensing with 2-aminopurine labeled DNAzymes

4.1 Introduction

Based on the activity study above, the new mutant of the NaA43 DNAzyme selected by our *in vitro* selection is highly sensitive and selective to Na^+ at pH 6. With 10 mM Na^+, CoH1 displayed a cleavage rate of ~0.07 min^{-1} in the gel-based assays. Having demonstrated its catalytic properties, we aimed to further apply the CoH1 in designing a Na^+-biosensor. So far, many strategies have been reported to design metal ion sensors using metal-specific DNAzymes.[28,80-82] For instance, a traditional DNAzyme-based fluorescent sensor is constructed by attaching a fluorophore/quencher pair to DNAzyme strands. The quencher group can eliminate the initial cleavage signal. The fluorophore is released and detected in the presence of metal ion targets. Following this strategy, Torabi *et al.* successfully converted the NaA43 DNAzyme into a fluorescent sensor for imaging Na^+ in live cells (Figure 4.1A).[69] This sensor exhibited a detection limit of 135 μM and a remarkable selectivity.

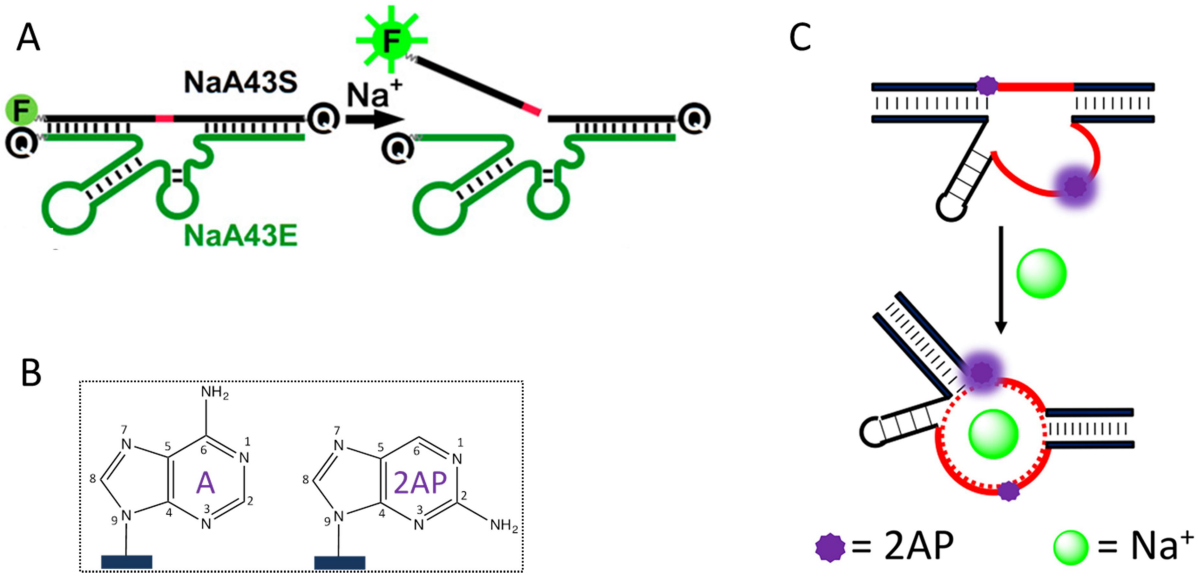

Figure 4.1 (A) Catalytic beacon design of the Na^+-dependent NaA43 DNAzyme. The substrate strand

(NaA43S) was labeled with a FAM at its 3′ end and a quencher at its 5′ end. The enzyme strand (NaA43E) was labeled with a second quencher at its 3′ end. Upon adding Na^+, the substrate was cleaved and released the fluorophore. (Adapted from ref. 69) Copyright © 2015 National Academy of Sciences (B) The chemical structures of an adenine and its analog, 2AP. (C) Two strategies of probing the Na^+-induced folding in Ce13d with 2AP. (Adapted from ref. 83) Copyright © 2016 Oxford University Press

Most recently, robust Na^+ sensing was achieved by probing a well-defined Na^+ aptamer with 2-aminopurine (2AP).[83] As described above, the Ce13d and NaA43 DNAzymes share a 16-nucleotide domain (Figure 3.2), which was demonstrated to be a highly selective and robust Na^+ aptamer in the subsequent biochemical studies. This is known to be the first well-defined metal binding domain found in the metal-specific DNAzymes. Based on Tb^{3+} luminescence and DMS (dimethyl sulfate) footprinting studies, the binding of Na^+ to this 16-nucleotide pocket induces a specific local folding of the Ce13d DNAzyme.[74,84]

A novel strategy of sensing Na^+ by detecting the metal-induced folding in a DNAzyme was developed using 2AP. 2AP is a fluorescent adenine analog with its chemical structure showing in Figure 4.1B. The emission intensity of 2AP highly depends on the local base-stacking interactions.[85] Figure 4.2A describes the base-stacking interactions in a DNA double helix. Apart from hydrogen bonding, base stacking also contributes to the duplex stability.[86-87] The fluorescence of 2AP is efficiently quenched by enhanced stacking interactions with neighbor bases, which could be recovered by relaxing the base stacking.[88] Taking advantages of this property, 2AP has been widely used as a powerful reporter of nucleic acid structure.[89-91]

For Na^+ sensing, a 2AP was introduced to the substrate strand by replacing the rA at the cleavage site. As shown in Figure 4.1C, the binding of Na^+ resulted in a relaxed base stacking around 2AP, and enhanced the emission in the meantime.[83] Using the wild-type Ce13d enzyme, the addition of 100 mM Na^+ induced a fluorescence increase of ~40% (Figure 4.2B, red trace).

Titrating the chloride salts of Rb^+ or Cs^+ led to a slight decrease in the signal. This may due to the increased ionic strength in the solution. High salt concentration can mask the repulsion force between two phosphodiester backbones. As for NaA43, the signal was increased by only ~20%. This difference was explained by the 5-nt motif in NaA43 which may modulate the stacking environment near 2AP. Moreover, a series of rational mutations were designed to improve the signal by at most 600%. A detection limit of 0.4 mM Na^+ was finally attained using an optimized sequence. On the other hand, replacing an adenine in the aptamer loop with 2AP resulted in a fluorescence quenching (Figure 4.1C). This indicates a more compact structure of the enzyme loop upon binding to Na^+.

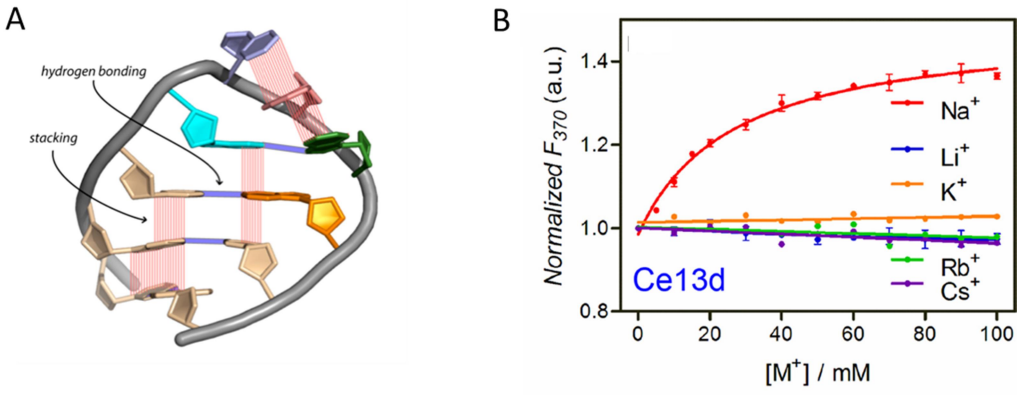

Figure 4.2 (A) The base-stacking interaction in a DNA double helix. (Adapted from ref. 86) (B) Normalized fluorescence intensity at 370 nm of the Ce13d DNAzyme as a function of metal ion concentration. (Adapted from ref. 83) Copyright © 2016 Oxford University Press

As a new mutant of NaA43, CoH1 also possesses the well-defined Na^+ aptamer in its catalytic loop. Instead of using a beacon design, 2AP probes were applied to CoH1 to achieve the folding-based Na^+ detection in this work. This will provide valuable information about the conformational change and reaction mechanism of CoH1 as well.

4.2 Na^+-induced folding of CoH1

First of all, we shortened the CoH1 enzyme to improve the duplex stability. Previous studies revealed that the role of a hairpin is to stabilize the structure which is unimportant for the activity. As a result, we shortened the hairpin structure in the wild-type CoH1 into the secondary structure in Figure 4.3A (in grey box). To confirm its activity, the cleavage reactions of both original and shortened CoH1 were carried out with 10 mM Na^+. As shown in Figure 4.3B, CoH1 with shortened hairpin structure still preserved its high cleavage activity. For better comparison, NaA43 with the same shortened hairpin structure was also used in the 2AP assays, whose activity was confirmed in a previous study reported by our group.[74]

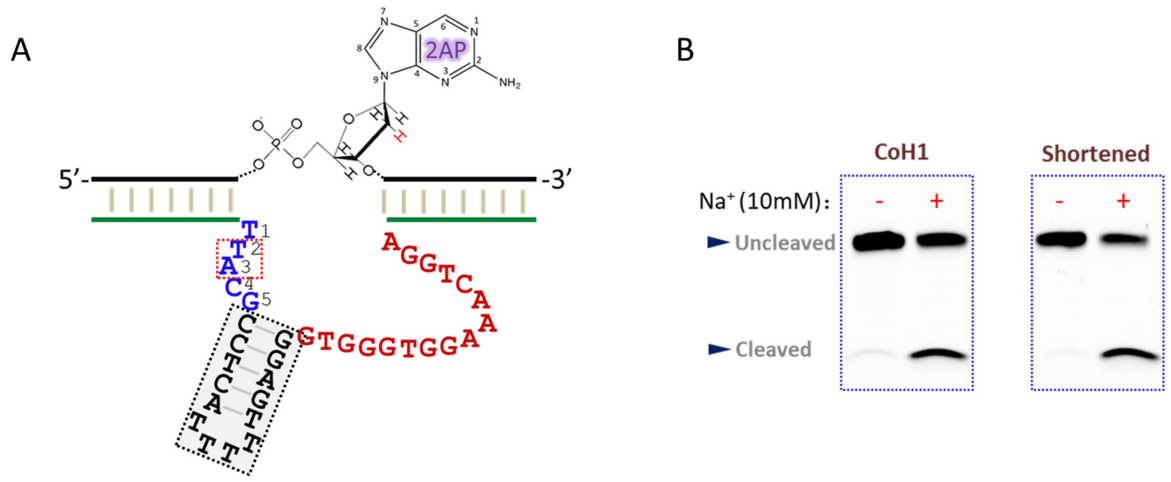

Figure 4.3 (A)The secondary structure of CoH1 with a shortened hairpin in the grey box. The 16-nt loop in red color represents the Na^+-binding domain. A deoxyri-2AP replaced the rA at the cleavage site. (B) Activity test of the wild-type and shortened CoH1 in the presence of 10 mM Na^+ for 30 min. The truncated hairpin structure maintained the cleavage activity.

To introduce probes into the DNAzyme, the rA at the cleavage site was replaced with a 2AP deoxyribonucleotide embedded in the substrate strand (Figure 4.3A). With an excitation at 310 nm, the CoH1 DNAzyme complex emits the peak intensity at ~370 nm (Figure 4.4, green

trace). With the addition of 100 mM Na^+, the emission intensity of CoH1 was improved by ~80% (red trace). This signal increase suggests that the base stacking between 2AP and its neighbor bases was relaxed upon binding with Na^+. In other words, the tertiary structure of the aptamer domain induced by Na^+ turns the 2AP site into a relatively more flexible state. As a comparison, the fluorescence of the NaA43 DNAzyme was measured (blue trace). The initial signal of CoH1 was higher than that of NaA43. This may due to the weak A-T base pair on the left side of the 2AP in CoH1 which leaves 2AP into a relatively loose state. The signal of NaA43 increased by 40% with 100 mM Na^+ (yellow trace).

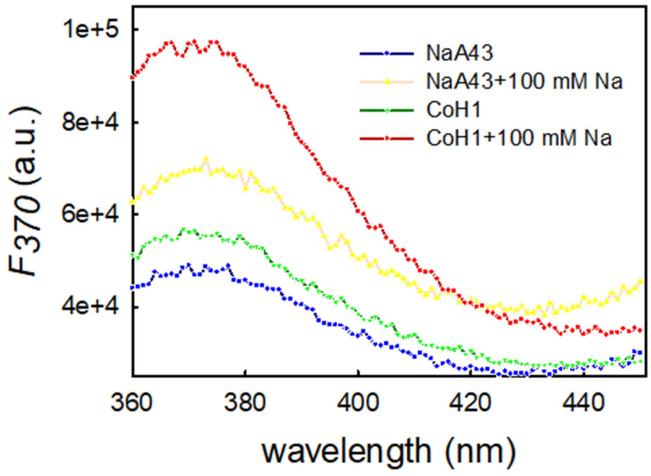

Figure 4.4 The fluorescence spectra of the CoH1 and NaA43 DNAzymes probed by 2AP with or without 100 mM Na^+. The emission wavelength ranges from 360 to 450 nm.

4.3 Sensitivity and selectivity

To test the sensitivity of 2AP-probed DNAzymes, sodium chloride was titrated gradually to achieve a final concentration of 100 mM Na^+. To normalize the signal, the peak intensity at 370 nm was divided by the initial fluorescence in the absence of Na^+. As shown in Figure 4.5A, the fluorescence signal increased with increasing Na^+ concentrations. After fitting the one-site

binding equation of $F = F_0 + a \cdot [M^+]/(k_d + [M^+])$, a dissociation constant (K_d) of 39 mM Na^+ was obtained. With 100 mM Na^+, a fluorescence enhancement of ~80% was reached. By contrast, only ~30% enhancement was observed for NaA43 with a K_d value of 66 mM. Due to their structural similarity, the 5-nt motif (blue colored) must be responsible for the higher enhancement observed in CoH1, which is more flexible and sensitive to the folding of Na^+ aptamer. Alternatively, the mutation of T_2A_3 in the 5-nt motif might facilitate the aptamer domain to bind Na^+ more strongly.

Moreover, the K_d value (39 mM Na^+) of CoH1 is fairly higher than the K_d (4.3 mM Na^+) obtained from previous activity assays. Several factors may contribute to such a difference. First, the low emission intensity of 2AP probes causes a significant signal noise in the spectra. Also, the fluorescence of 2AP highly depends on its aqueous environment. For example, an increasing ionic strength caused by the Na^+ titration tends to decrease the fluorescence. Since folding-based method is less sensitive than the cleavage-based method, we proposed that the folding of the aptamer loop might not fully reflect the catalysis of the DNAzyme. In other words, other parts of CoH1, such as the 5-nt motif, also play a critical role in the cleavage reaction apart from the folding of the aptamer. In addition, the range of 0-20 mM was plotted in Figure 4.4B. A linear relationship was obtained with a detection limit of 3.0 mM Na^+. The detection limit was calculated from 3σ/slope, where σ is the standard deviation of background signal.

As discussed above, the linear response obtained from the gel-based activity assays is below 1.5 mM Na^+. Herein, the linear Na^+ response of the folding-based sensors is wider and more robust. The decreased sensitivity is likely due to the low emission intensity of 2AP. In addition, in the cleavage assay, each Na^+ might participate in the cleavage of multiple DNAzymes with catalytic turnovers. We propose that Na^+ binding to the aptamer domain is

necessary for the activity. The folding of the aptamer loop relaxes the base stacking at the cleavage site, which creates a ready-to-go state for the reaction to start. However, those 5 nucleotides on the left side of the hairpin are responsible for directly participating into the reaction. Especially, T_2 and A_3 bases (Figure 4.3, red box) are critical and determine the reaction rate to a great extent based on mutation studies. This conclusion is consistent with previous study on NaA43 in which G_{23} turned out to be important for its catalysis.[74]

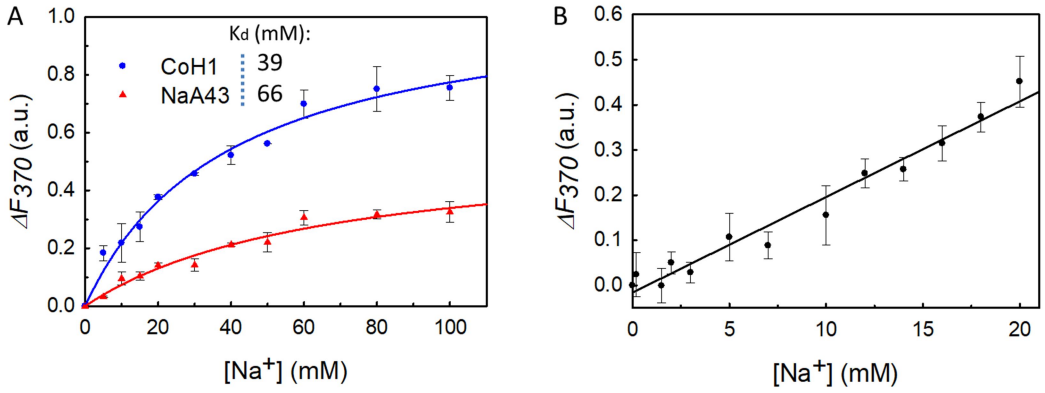

Figure 4.5 (A) Normalized fluorescence intensity at 370 nm of the CoH1 and NaA43 as a function of Na^+ concentration. (B) The linear response appeared between 0 to 20 mM Na^+. A detection limit of 3.0 mM Na^+ was obtained. The emission intensity enhancement at 370 nm was normalized by equation F/F_0-1. F_0 and F represent the fluorescence signal before and after the addition of Na^+, respectively.

Next, the sensor specificity was tested by comparing with other competing monovalent ions in group 1A. As seen in Figure 4.6, only Na^+ induced a fluorescence increase of ~60% with a concentration of 50 mM (green bars). With the addition of 100 mM metals, only Cs^+ showed a weak response while all the other ions made negligible change on the signal (red bars). Meanwhile, ~80% enhancement was induced with 100 mM Na^+ suggesting a high selectivity of the 2AP sensor.

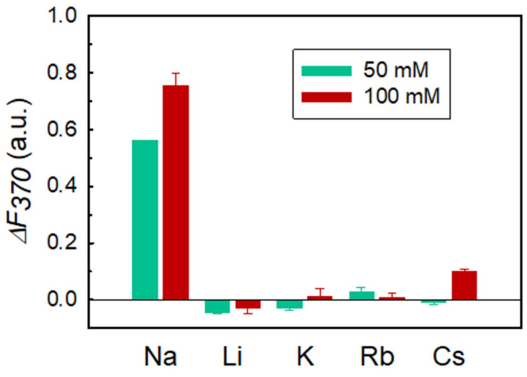

Figure 4.6 The selectivity test of the 2AP sensor in the presence of 50 mM or 100 mM various monovalent ions.

4.4 Materials and methods

4.4.1 Chemicals

The deoxyribo-2AP-modified substrate, shortened CoH1, and NaA43 enzymes were purchased from Integrated DNA Technologies (Coralville, IA, USA). Table 4 lists all the DNA sequences and modifications. All the metal salts including sodium chloride, lithium chloride potassium chloride, rubidium chloride, and cesium chloride, along with all the buffers were described in the last chapter. Milli-Q water was used to prepare all the buffers and solutions.

DNA name	Sequences and modifications
Sub-deoxyribo-2AP	5'-GTCACGAGTCACTAT[2AP]GGAAGATGGCGAAA
CoH1 (shortened)	5'-TTTCGCCATAGGTCAAAGGTGGGTGGGAGTTTTTACTCCGCATTAGTGACTCGTGAC
NaA43 (shortened)	5'-TTTCGCCATCCAGGTCAAAGGTGGGTGAGGAGTTTTTACTCCGCGGTTAGTGACTCGTGAC

Table 4. DNA oligonucleotides and their modifications used in the 2AP assays. [2AP] = 2-aminopurine.

4.4.2 Fluorescence spectroscopy

First, the DNAzyme complexes (1 μM) were prepared by annealing in buffer B (50 mM MES, pH 6, 25 mM LiCl). The ratio of 2AP-modified substrates and enzyme strands was 1:2. The mixture was heated in 80°C water and followed by gradual cooling down to 4°C for at least 30 min. The fluorescence spectra were measured using a fluorometer (FluoroMax-4, Horiba Scientific). With an excitation at 310 nm, the emission intensity was measured from 360 to 450 nm. For each measurement, a small volume (<1.0 μL) of metal salts was titrated into the sample to achieve an intended concentration. After a quick mix, the fluorescence was measure as soon as possible. The emission intensity at 370 nm was always used for quantification. The emission intensity enhancement at 370 nm was normalized by equation F/F_0-1. F_0 and F represent the fluorescence signal before and after the addition of Na^+, respectively. The K_d value was obtained by fitting into the one-site binding equation: $F = F_0 + a \cdot [M^+]/(k_d + [M^+])$. $[M^+]$ is the metal concentration, and a is the fluorescence change when $[M^+] = \infty$.

4.4.3 Gel-based assays

To confirm the cleavage activity of the shortened CoH1, the DNAzyme complexes were prepared with either wild-type or shortened CoH1 enzymes. The reactions were carried out with 10 mM NaCl at room temperature. After 30 min, the reaction was quenched with the addition of 8 M Urea (8 μL). The reaction products were separated by 15% dPAGE (200V, for 1 h 20 min) and analyzed by a Bio-Rad ChemiDoc MP imaging system.

Chapter 5. Conclusions and future work

In summary, active DNAzyme sequences were enriched and isolated after 6 rounds of *in vitro* selection at pH 6. Although the selection used $Co(NH_3)_6^{3+}$ as the intended cofactor, this selected representative sequence (CoH1) showed catalytic activity in the presence of Na^+ only, while $Co(NH_3)_6^{3+}$ acted as an inhibitor. The secondary structure prediction of the CoH1 revealed a well-defined Na^+ binding domain in its catalytic core, which explained the Na^+-dependent activity. In particular, the structure of CoH1 was found to be highly similar to the previously reported Na^+-dependent DNAzyme, NaA43. However, two nucleotides in the NaA43 that are known to be critical for its activity mutated into T_2A_3 in the CoH1. Further mutation studies indicated that any mutation to T_2 or A_3 may completely abolish the activity of CoH1. One of the future directions is to perform more mutation studies to provide a detailed picture of its catalytic mechanism.

As a new mutant of NaA43, CoH1 exhibited distinct catalytic activity in the gel-based studies. With 10 mM Na^+, CoH1 displays a fast cleavage rate of ~0.07 min^{-1}, which is 3.5-fold higher than NaA43 at the same Na^+ concentration. Under its optimal condition (50 mM MES, pH 6, 25 mM LiCl), CoH1 has a stronger binding affinity toward Na^+ with a K_d value of 4.3 ± 0.6 mM Na^+. In conclusion, CoH1 shows a great potential in Na^+ detection at low concentrations. Based on our results, pH is important for distinguishing CoH1 from NaA43. Overall, CoH1 displays higher cleavage activity at pH below ~6.5, while NaA43 is more active at higher pH. It is interesting to note that two-site mutations in the 5-nt motif resulted in distinct pH-dependent activities. From the biochemistry aspects, future efforts can be paid in studying the pH-dependent evolution of the 5-nt motif. Due to the critical role of these 5 nucleotides, a DNA library containing a fixed hairpin, the Na^+ binding domain, and a 5-nt motif with random

sequences could be designed for future selections. By tuning the selection conditions (e.g., pH, ionic strength, metal ions), new mutants with distinct properties could be discovered.

Finally, 2AP probes were applied to convert the CoH1 DNAzyme into a folding-based Na^+ sensor. The sensor displays a linear respond below 20 mM with a detection limit of 3.0 mM Na^+. In the presence of 100 mM Na^+, ~80% enhancement was observed in the Na^+ sensor with a high selectivity over other monovalent ions. The 2AP probes revealed the Na^+-induced folding of the Na^+ aptamer and provided important insights to the reaction mechanism. To improve the fluorescence signal, rational mutations can be performed to CoH1. For example, a double mutation of $C_{10}A_{20}$ was demonstrated to enhance the signal by 600% in Ce13d.[17] Ultimately, the optimized sensor could be applied for real-time Na^+ detection in live cells. In the subsequent work, replacing A_3 in the 5 nt-motif with 2AP may reveal the local folding of the 5-nt motif. This strategy can be followed to study more metal-binding domains in other metal-specific DNAzymes.

Chapter 6. Lab Safety

General laboratory safety practices should always be followed during experiments. This includes wearing gloves, goggles and a lab coat. Material safety data sheets should also be referred to routinely. In particular, toxic chemicals should be stored appropriately and handled carefully. Ethidium bromide may be used to stain the gel and locate the DNA. This is a potential mutagen and carcinogen, and will therefore be handled with caution. During preparation and handling, nitrile gloves will be worn as well as a lab coat. Handling of this solution will be carried out inside a chemical fume hood to prevent exposure. All waste that comes into contact with ethidium bromide, as well as the solution after use will be collected in a specially marked container and brought down to ESC-150 (Environmental Safety Facility) for disposal.

Precautions to prevent electrical shock must be taken to use electrophoresis apparatus safely. The power must be turned off before connecting the electrical leads. Hands must be dry before connecting the leads. The equipment should always be kept away from sinks or other water sources.

References

(1) Kruger, K.; Grabowski, P. J.; Zaug, A. J.; Sands, J.; Gottschling, D. E.; Cech, T. R. Self-Splicing RNA: Autoexcision and Autocyclization of the Ribosomal RNA Intervening Sequence of Tetrahymena. *Cell* **1982,** *31*, 147-157.

(2) Prody, G. A.; Bakos, J. T.; Buzayan, J. M.; Schneider, I. R.; Bruening, G. Autolytic Processing of Dimeric Plant Virus Satellite Rna. *Science* **1986,** *231*, 1577-1580.

(3) Doudna, J. A.; Cech, T. R. The Chemical Repertoire of Natural Ribozymes. *Nature* **2002,** *418*, 222-228.

(4) Ban, N.; Nissen, P.; Hansen, J.; Moore, P. B.; Steitz, T. A. The Complete Atomic Structure of the Large Ribosomal Subunit at 2.4 Å Resolution. *Science* **2000,** *289*, 905-920.

(5) Breaker, R. R.; Joyce, G. F. A DNA Enzyme That Cleaves RNA. *Chemistry & Biology* **1994,** *1*, 223-229.

(6) Santoro, S. W.; Joyce, G. F.; Sakthivel, K.; Gramatikova, S.; Barbas, C. F. RNA Cleavage by a DNA Enzyme with Extended Chemical Functionality. *Journal of the American Chemical Society* **2000,** *122*, 2433-2439.

(7) Carmi, N.; Balkhi, S. R.; Breaker, R. R. Cleaving DNA with DNA. *Proceedings of the National Academy of Sciences of the United States of America* **1998,** *95*, 2233-2237.

(8) Purtha, W. E.; Coppins, R. L.; Smalley, M. K.; Silverman, S. K. General Deoxyribozyme-Catalyzed Synthesis of Native 3'-5' RNA Linkages. *Journal of the American Chemical Society* **2005,** *127*, 13124-13125.

(9) Li, Y.; Breaker, R. R. Phosphorylating DNA with DNA. *Proceedings of the National Academy of Sciences* **1999,** *96*, 2746-2751.

(10) Li, Y.; Liu, Y.; Breaker, R. R. Capping DNA with DNA. *Biochemistry* **2000,** *39*, 3106-3114.

(11) Santoro, S. W.; Joyce, G. F. A General Purpose RNA-Cleaving DNA Enzyme. *Proceedings of the National Academy of Sciences* **1997,** *94*, 4262-4266.

(12) Faulhammer, D.; Famulok, M. The Ca^{2+} Ion as a Cofactor for a Novel RNA-Cleaving Deoxyribozyme. *Angewandte Chemie International Edition* **1996,** *35*, 2837-2841.

(13) Li, J.; Zheng, W.; Kwon, A. H.; Lu, Y. *In Vitro* Selection and Characterization of a Highly Efficient Zn (II)-Dependent RNA-Cleaving Deoxyribozyme. *Nucleic acids research* **2000,** *28*, 481-488.

(14) Cruz, R. P.; Withers, J. B.; Li, Y. Dinucleotide Junction Cleavage Versatility of 8-17 Deoxyribozyme. *Chemistry & biology* **2004,** *11*, 57-67.

(15) Liu, J.; Brown, A. K.; Meng, X.; Cropek, D. M.; Istok, J. D.; Watson, D. B.; Lu, Y. A Catalytic Beacon Sensor for Uranium with Parts-Per-Trillion Sensitivity and Millionfold Selectivity. *Proceedings of the National Academy of Sciences* **2007,** *104*, 2056-2061.

(16) Brown, A. K.; Liu, J.; He, Y.; Lu, Y. Biochemical Characterization of a Uranyl Ion-Specific DNAzyme. *ChemBioChem* **2009,** *10*, 486-492.

(17) Huang, P.-J. J.; Lin, J.; Cao, J.; Vazin, M.; Liu, J. Ultrasensitive DNAzyme Beacon for Lanthanides and Metal Speciation. *Analytical Chemistry* **2014,** *86*, 1816-1821.

(18) Huang, P.-J. J.; Vazin, M.; Liu, J. *In Vitro* Selection of a New Lanthanide-Dependent DNAzyme for Ratiometric Sensing Lanthanides. *Analytical Chemistry* **2014,** *86*, 9993-9999.

(19) Huang, P.-J. J.; Vazin, M.; Liu, J. *In Vitro* Selection of a DNAzyme Cooperatively Binding Two Lanthanide Ions for RNA Cleavage. *Biochemistry* **2016,** *55*, 2518-2525.

(20) Silverman, S. K. Catalytic DNA (Deoxyribozymes) for Synthetic Applications-Current Abilities and Future Prospects. *Chemical Communications* **2008**, 3467-3485.

(21) DeRose, V. J. Metal Ion Binding to Catalytic RNA Molecules. *Current Opinion in Structural Biology* **2003,** *13*, 317-324.

(22) Santoro, S. W.; Joyce, G. F. Mechanism and Utility of an RNA-Cleaving DNA Enzyme. *Biochemistry* **1998,** *37*, 13330-13342.

(23) Ward, W. L.; Plakos, K.; DeRose, V. J. Nucleic Acid Catalysis: Metals, Nucleobases, and Other Cofactors. *Chemical Reviews* **2014,** *114*, 4318-4342.

(24) Wirmer - Bartoschek, J.; Schwalbe, H. Understanding How DNA Enzymes Work. *Angewandte Chemie International Edition* **2016,** *55*, 5376-5377.

(25) Takagi, Y.; Warashina, M.; Stec, W. J.; Yoshinari, K.; Taira, K. Survey and Summary: Recent Advances in the Elucidation of the Mechanisms of Action of Ribozymes. *Nucleic acids research* **2001,** *29*, 1815-1834.

(26) Willner, I.; Shlyahovsky, B.; Zayats, M.; Willner, B. DNAzymes for Sensing, Nanobiotechnology and Logic Gate Applications. *Chemical Society Reviews* **2008,** *37*, 1153-1165.

(27) Lu, Y.; Liu, J. Functional DNA Nanotechnology: Emerging Applications of DNAzymes and Aptamers. *Current opinion in biotechnology* **2006,** *17*, 580-8.

(28) Liu, J.; Cao, Z.; Lu, Y. Functional Nucleic Acid Sensors. *Chemical Reviews* **2009,** *109*, 1948-1998.

(29) Cutler, J. I.; Auyeung, E.; Mirkin, C. A. Spherical Nucleic Acids. *Journal of the American Chemical Society* **2012,** *134*, 1376-1391.

(30) Li, J.; Lu, Y. A Highly Sensitive and Selective Catalytic DNA Biosensor for Lead Ions. *Journal of the American Chemical Society* **2000,** *122*, 10466-10467.

(31) Wang, Y.; Silverman, S. K. Efficient One-Step Synthesis of Biologically Related Lariat Rnas by a Deoxyribozyme. *Angewandte Chemie* **2005,** *44*, 5863-6.

(32) Gao, X.; Huang, H.; Niu, S.; Ye, H.; Lin, Z.; Qiu, B.; Chen, G. Determination of Magnesium Ion in Serum Samples by a DNAzyme-Based Electrochemical Biosensor. *Analytical Methods* **2012,** *4*, 947.

(33) Liu, M.; Zhao, H.; Chen, S.; Yu, H.; Zhang, Y.; Quan, X. A "Turn-on" Fluorescent Copper Biosensor Based on DNA Cleavage-Dependent Graphene-Quenched DNAzyme. *Biosensors & bioelectronics* **2011,** *26*, 4111-6.

(34) Lu, Y. New Transition-Metal-Dependent DNAzymes as Efficient Endonucleases and as Selective Metal Biosensors. *Chemistry - A European Journal* **2002,** *8*, 4588-96.

(35) Luo, Y.; Zhang, Y.; Xu, L.; Wang, L.; Wen, G.; Liang, A.; Jiang, Z. Colorimetric Sensing of Trace $UO_2(2+)$ by Using Nanogold-Seeded Nucleation Amplification and Label-Free DNAzyme Cleavage Reaction. *The Analyst* **2012,** *137*, 1866-71.

(36) Liu, J.; Lu, Y. A Colorimetric Lead Biosensor Using DNAzyme-Directed Assembly of Gold Nanoparticles. *Journal of the American Chemical Society* **2003,** *125*, 6642-6643.

(37) Wilson, D. S. ; Szostak, J. W. *In Vitro* Selection of Functional Nucleic Acids. *Annual Review of Biochemistry* **1999,** *68*, 611-647.

(38) Drolet, D. W.; Moon-McDermott, L.; Romig, T. S. An Enzyme-Linked Oligonucleotide Assay. *Nature biotechnology* **1996,** *14*, 1021-1025.

(39) Lin, Y.; Nieuwlandt, D.; Magallanez, A.; Feistner, B.; Jayasena, S. D. High-Affinity and Specific Recognition of Human Thyroid Stimulating Hormone (HTSH) by *in Vitro*-Selected 2'-Amino-Modified RNA. *Nucleic Acids Research* **1996,** *24*, 3407-3414.

(40) Pan, T.; Uhlenbeck, O. C. A Small Metalloribozyme with a Two-Step Mechanism. *Nature* **1992,** *358*, 560-563.

(41) Bartel, D.; Szostak, J. Isolation of New Ribozymes from a Large Pool of Random Sequences. *Science* **1993,** *261*, 1411-1418.

(42) Wilson, C.; Szostak, J. W. *In Vitro* Evolution of a Self-Alkylatlng Ribozyme. *Nature* **1995,** *374*, 777-782.

(43) Sassanfar, M.; Szostak, J. W. An RNA Motif That Binds ATP. *Nature* **1993,** *364*, 550-553.

(44) Breaker, R. R. *In Vitro* Selection of Catalytic Polynucleotides. *Chemical Reviews* **1997,** *97*, 371-390.

(45) Silverman, S. K. *In Vitro* Selection, Characterization, and Application of Deoxyribozymes That Cleave RNA. *Nucleic Acids Research* **2005,** *33*, 6151-6163.

(46) Li, J.; Zheng, W.; Kwon, A. H.; Lu, Y. *In Vitro* Selection and Characterization of a Highly Efficient Zn(II)-Dependent RNA-Cleaving Deoxyribozyme. *Nucleic Acids Research* **2000,** *28*, 481-488.

(47) Huang, P.-J. J.; Liu, J. Rational Evolution of Cd^{2+}-Specific DNAzymes with Phosphorothioate Modified Cleavage Junction and Cd^{2+} Sensing. *Nucleic Acids Research* **2015,** *43*, 6125-6133.

(48) Bruesehoff, P. J.; Li, J.; Augustine Iii, A. J.; Lu, Y. Improving Metal Ion Specificity During *in Vitro* Selection of Catalytic DNA. *Combinatorial Chemistry & High Throughput Screening* **2002,** *5*, 327-335.

(49) Cowan, J. A. Metallobiochemistry of RNA. $Co(NH_3)_6^{3+}$ as a Probe for Mg^{2+}(aq) Binding Sites. *Journal of Inorganic Biochemistry* **1993,** *49*, 171-175.

(50) Crabtree, R. H. Metal Ions at Work. *Science* **1994,** *266*, 1591-1592.

(51) Kim, S.; Cowan, J. A. Inert Cobalt Complexes as Mechanistic Probes of the Biochemistry of Magnesium Cofactors. Application to Topoisomerase I. *Inorganic Chemistry* **1992,** *31*, 3495-3496.

(52) Kieft, J. S.; Tinoco, I., Jr. Solution Structure of a Metal-Binding Site in the Major Groove of RNA Complexed with Cobalt (III) Hexammine. *Structure 5*, 713-721.

(53) Kieltyka, J. W.; Chow, C. S. Probing RNA Hairpins with Cobalt(III)Hexammine and Electrospray Ionization Mass Spectrometry. *Journal of the American Society for Mass Spectrometry* **2006,** *17*, 1376-1382.

(54) Widom, J.; Baldwin, R. L. Monomolecular Condensation of λ-DNA Induced by Cobalt Hexammine. *Biopolymers* **1983,** *22*, 1595-1620.

(55) Ouameur, A. A.; Tajmir-Riahi, H.-A. Structural Analysis of DNA Interactions with Biogenic Polyamines and Cobalt(III)Hexamine Studied by Fourier Transform Infrared and Capillary Electrophoresis. *Journal of Biological Chemistry* **2004,** *279*, 42041-42054.

(56) Cheatham, T. E., III; Kollman, P. A. Insight into the Stabilization of a-DNA by Specific Ion Association: Spontaneous B-DNA to a-DNA Transitions Observed in Molecular Dynamics Simulations of D[ACCCGCGGT] in the Presence of Hexaamminecobalt(III). *Structure 5*, 1297-1311.

(57) Wilson, T. J.; Lilley, D. M. J. Metal Ion Binding and the Folding of the Hairpin Ribozyme. *RNA* **2002,** *8*, 587-600.

(58) Hampel, A.; Cowan, J. A. A Unique Mechanism for RNA Catalysis: The Role of Metal Cofactors in Hairpin Ribozyme Cleavage. *Chemistry & Biology* **1997,** *4*, 513-517.

(59) Rangan, P.; Woodson, S. A. Structural Requirement for Mg^{2+} Binding in the Group I Intron Core. *Journal of Molecular Biology* **2003,** *329*, 229-238.

(60) Horton, T. E.; DeRose, V. J. Cobalt Hexammine Inhibition of the Hammerhead Ribozyme. *Biochemistry* **2000,** *39*, 11408-11416.

(61) Maguire, J. L.; Collins, R. A. Effects of Cobalt Hexammine on Folding and Self-Cleavage of the Neurospora *Vs* Ribozyme1. *Journal of Molecular Biology* **2001,** *309*, 45-56.

(62) Nesbitt, S.; Hegg, L. A.; Fedor, M. J. An Unusual pH-Independent and Metal-Ion-Independent Mechanism for Hairpin Ribozyme Catalysis. *Chemistry & Biology* **1997,** *4*, 619-630.

(63) Feldman, A. R.; Leung, E. K. Y.; Bennet, A. J.; Sen, D. The RNA-Cleaving Bipartite Dnazyme Is a Distinctive Metalloenzyme. *ChemBioChem* **2006,** *7*, 98-105.

(64) Kauffman, G. B.; Sugisaka, N.; Emerson, K.; Bares, L. A.; Houk, C. C. Hexaamminecobalt(III) Chloride. In *Inorganic Syntheses*; John Wiley & Sons, Inc., 2007, pp 157-160.

(65) Repo, E.; Warchoł, J. K.; Bhatnagar, A.; Mudhoo, A.; Sillanpää, M. Aminopolycarboxylic Acid Functionalized Adsorbents for Heavy Metals Removal from Water. *Water Research* **2013,** *47*, 4812-4832.

(66) Zuker, M. Mfold Web Server for Nucleic Acid Folding and Hybridization Prediction. *Nucleic acids research* **2003,** *31*, 3406-3415.

(67) Zuker, M.; Jacobson, A. B. Using Reliability Information to Annotate RNA Secondary Structures. *RNA* **1998,** *4*, 669-679.

(68) Brown, A. K.; Li, J.; Pavot, C. M.-B.; Lu, Y. A Lead-Dependent DNAzyme with a Two-Step Mechanism. *Biochemistry* **2003,** *42*, 7152-7161.

(69) Torabi, S.-F.; Wu, P.; McGhee, C. E.; Chen, L.; Hwang, K.; Zheng, N.; Cheng, J.; Lu, Y. *In Vitro* Selection of a Sodium-Specific DNAzyme and Its Application in Intracellular Sensing. *Proceedings of the National Academy of Sciences* **2015,** *112*, 5903-5908.

(70) Sigel, A.; Sigel, H.; Sigel, R. K. *Interrelations between Essential Metal Ions and Human Diseases*; Springer **2013**.

(71) Murray, R. K. Harper's Illustrated Biochemistry. **2009**.

(72) Lee, J. J. Y.; Kilonzo, K.; Nistico, A.; Yeates, K. Management of Hyponatremia. *Canadian Medical Association Journal* **2014,** *186*, E281-E286.

(73) Zhou, W.; Saran, R.; Chen, Q.; Ding, J.; Liu, J. A New Na^+-Dependent RNA-Cleaving DNAzyme with over 1000-Fold Rate Acceleration by Ethanol. *ChemBioChem* **2016,** *17*, 159-163.

(74) Zhou, W.; Zhang, Y.; Huang, P.-J. J.; Ding, J.; Liu, J. A DNAzyme Requiring Two Different Metal Ions at Two Distinct Sites. *Nucleic acids research* **2016,** *44*, 354-363.

(75) Torabi, S.-F.; Lu, Y. Identification of the Same Na^+-Specific DNAzyme Motif from Two *in Vitro* Selections under Different Conditions. *Journal of Molecular Evolution* **2015,** *81*, 225-234.

(76) Tannock, I. F.; Rotin, D. Acid pH in Tumors and Its Potential for Therapeutic Exploitation. *Cancer research* **1989,** *49*, 4373-4384.

(77) Iamshanova, O.; Mariot, P.; Lehen'Kyi, V. Y.; Prevarskaya, N. Comparison of Fluorescence Probes for Intracellular Sodium Imaging in Prostate Cancer Cell Lines. *European Biophysics Journal* **2016,** *45*, 765-777.

(78) Saran, R.; Liu, J. A Silver DNAzyme. *Analytical chemistry* **2016,** *88*, 4014-4020.

(79) Albright, L. M.; Slatko, B. E. Denaturing Polyacrylamide Gel Electrophoresis. In *Current Protocols in Human Genetics*; John Wiley & Sons, Inc., 2001.

(80) Zhang, X.-B.; Kong, R.-M.; Lu, Y. Metal Ion Sensors Based on DNAzymes and Related DNA Molecules. *Annual review of analytical chemistry* **2011,** *4*, 105-128.

(81) Kosman, J.; Juskowiak, B. Peroxidase-Mimicking DNAzymes for Biosensing Applications: A Review. *Analytica chimica acta* **2011,** *707*, 7-17.

(82) Zhou, Y.; Tang, L.; Zeng, G.; Zhang, C.; Zhang, Y.; Xie, X. Current Progress in Biosensors for Heavy Metal Ions Based on DNAzymes/DNA Molecules Functionalized Nanostructures: A Review. *Sensors and Actuators B: Chemical* **2016,** *223*, 280-294.

(83) Zhou, W.; Ding, J.; Liu, J. A Highly Specific Sodium Aptamer Probed by 2-Aminopurine for Robust Na^+ Sensing. *Nucleic acids research* **2016,** *44*, 10377-10385.

(84) Vazin, M.; Huang, P.-J. J.; Matuszek, Z. a.; Liu, J. Biochemical Characterization of a Lanthanide-Dependent DNAzyme with Normal and Phosphorothioate-Modified Substrates. *Biochemistry* **2015,** *54*, 6132-6138.

(85) Jean, J. M.; Hall, K. B. 2-Aminopurine Fluorescence Quenching and Lifetimes: Role of Base Stacking. *Proceedings of the National Academy of Sciences* **2001,** *98*, 37-41.

(86) Williams, L. D. Yin and Yang: Polypeptide and Polynucleotide. *Origins of LIfe Community Page* **2012**.

(87) Hunter, C. A. Sequence-Dependent DNA Structure: The Role of Base Stacking Interactions. *Journal of molecular biology* **1993,** *230*, 1025-1054.

(88) Jones, A. C.; Neely, R. K. 2-Aminopurine as a Fluorescent Probe of DNA Conformation and the DNA–Enzyme Interface. *Quarterly reviews of biophysics* **2015,** *48*, 244-279.

(89) Saran, R.; Yao, L.; Hoang, P.; Liu, J. Folding of the Silver Aptamer in a DNAzyme Probed by 2-Aminopurine Fluorescence. *Biochimie* **2017**, *in press*.

(90) Rachofsky, E. L.; Osman, R.; Ross, J. A. Probing Structure and Dynamics of DNA with 2-Aminopurine: Effects of Local Environment on Fluorescence. *Biochemistry* **2001,** *40*, 946-956.

(91) Zhou, W.; Ding, J.; Liu, J. 2-Aminopurine-Modified DNA Homopolymers for Robust and Sensitive Detection of Mercury and Silver. *Biosensors and Bioelectronics* **2017,** *87*, 171-177.